The linear ubiquitin assembly complex (LUBAC) is essential for NLRP3 inflammasome activation

Mary A. Rodgers,[1] James W. Bowman,[1] Hiroaki Fujita,[2] Nicole Orazio,[1] Mude Shi,[1] Qiming Liang,[1] Rina Amatya,[1] Thomas J. Kelly,[1] Kazuhiro Iwai,[2] Jenny Ting,[3] and Jae U. Jung[1]

[1]Department of Molecular Microbiology and Immunology, Keck School of Medicine, University of Southern California, Los Angeles, CA 90033
[2]Department of Molecular and Cellular Physiology, Graduate School of Medicine, Kyoto University, Sakyo-ku, Kyoto 606-8501, Japan
[3]Department of Microbiology-Immunology, Lineberger Comprehensive Cancer Center, Center for Translational Immunology and Institute for Inflammatory Diseases, University of North Carolina at Chapel Hill, Chapel Hill, NC 27599

Linear ubiquitination is a newly discovered posttranslational modification that is currently restricted to a small number of known protein substrates. The linear ubiquitination assembly complex (LUBAC), consisting of HOIL-1L, HOIP, and Sharpin, has been reported to activate NF-κB–mediated transcription in response to receptor signaling by ligating linear ubiquitin chains to Nemo and Rip1. Despite recent advances, the detailed roles of LUBAC in immune cells remain elusive. We demonstrate a novel HOIL-1L function as an essential regulator of the activation of the NLRP3/ASC inflammasome in primary bone marrow–derived macrophages (BMDMs) independently of NF-κB activation. Mechanistically, HOIL-1L is required for assembly of the NLRP3/ASC inflammasome and the linear ubiquitination of ASC, which we identify as a novel LUBAC substrate. Consequently, we find that HOIL-1L$^{-/-}$ mice have reduced IL-1β secretion in response to in vivo NLRP3 stimulation and survive lethal challenge with LPS. Together, these data demonstrate that linear ubiquitination is required for NLRP3 inflammasome activation, defining the molecular events of NLRP3 inflammasome activation and expanding the role of LUBAC as an innate immune regulator. Furthermore, our observation is clinically relevant because patients lacking HOIL-1L expression suffer from pyogenic bacterial immunodeficiency, providing a potential new therapeutic target for enhancing inflammation in immunodeficient patients.

CORRESPONDENCE
Jae U. Jung:
jaeujung@med.usc.edu

Abbreviations used: BMDM, BM-derived macrophage; CoZi, coiled zipper; dsDNA, double-stranded DNA; FLICA, FAM-YVAD-FMK; IP, immunoprecipitation; LUBAC, linear ubiquitin assembly complex; MDP, muramyl dipeptide; MEF, mouse embryonic fibroblast; MSU, monosodium urate crystals; NZF, Npl4 type-zinc-finger; PRR, pattern recognition receptor; qPCR, quantitative PCR; RBR, RING between RING; UBL, ubiquitin like.

The innate immune response is precisely gated by regulatory mechanisms during both detection of a threat to the host and also the resulting responses. Such control is essential for preventing inappropriate or prolonged innate immune responses, which may damage the host as much as the pathogen or damaging signal itself. Specifically, posttranslational modification of substrate proteins by ubiquitination has been reported for many targets in innate immune signaling pathways as a mechanism of regulating their functions. The diversity of effects on target protein degradation, binding partner affinity, or localization resulting from ubiquitination modification is dependent on the lysine linkage position and length of the ubiquitin chain attached by a ubiquitin ligase enzyme. As a central pathway downstream from many innate and adaptive immune receptors, the NF-κB signaling pathway is highly regulated by lysine 48 (K48), K63, and linear ubiquitination modifications that are required for the ultimate release of the p50/p65 NF-κB transcription factor to the nucleus where it can turn on the expression of proinflammatory genes (Iwai and Tokunaga, 2009). After receptor stimulation by CD40 ligand, TNF, or IL-1β, the cIAP-mediated K63 ubiquitination of Rip1 or TRAF6 leads to recruitment of the linear ubiquitin assembly complex (LUBAC), consisting of HOIP and HOIL-1L or Sharpin,

The Rockefeller University Press $30.00
J. Exp. Med. 2014 Vol. 211 No. 7 1333-1347
www.jem.org/cgi/doi/10.1084/jem.20132486

The Journal of Experimental Medicine

or both (Haas et al., 2009). LUBAC is required for the linear ubiquitination of Rip1 and Nemo, resulting in the activation of the IKK kinase (Iwai and Tokunaga, 2009). Phosphorylation of IκBα by IKK is required for the K48 ubiquitination of IκBα, which leads to proteasomal degradation of IκBα and release of the p50/p65 NF-κB transcription factor for translocation to the nucleus (Iwai and Tokunaga, 2009). Although many protein substrates have been described for K48 and K63 ubiquitination, few have been described for linear ubiquitination, with only Rip1 and Nemo being the best characterized. Negative regulators of linear ubiquitination-dependent NF-κB activation have recently been reported, including the FAM105B (otulin) and CYLD linear ubiquitin-specific deubiquitinases (DUBs) and A20, which specifically binds the linear ubiquitin moiety and edits Rip1 ubiquitination to inhibit its activation (Wertz et al., 2004; Tokunaga et al., 2012; Verhelst et al., 2012; Keusekotten et al., 2013; Rivkin et al., 2013).

Because many receptor signaling pathways converge on Nemo activation, linear ubiquitination is expected to be required for the NF-κB–dependent gene expression of various pattern recognition receptor (PRR) pathways. Indeed, TLRs, such as TLR2, 3, 4, 7/8, and 9, have been shown to require LUBAC for NF-κB–dependent gene expression due to the linear ubiquitination of Nemo (Zak et al., 2011). The NOD2 (nucleotide-binding oligomerization domain-containing protein 2)-dependent activation of NF-κB in response to muramyl dipeptide (MDP) also requires LUBAC, which is recruited by the XIAP-mediated K63 ubiquitination of RIPK2 (Damgaard et al., 2012). In contrast, the HOIL-1L subunit of LUBAC is a negative regulator of the RIG-I intracellular virus-sensing PRR that competitively binds RIG-I and targets TRIM25 for degradation, thus stopping the TRIM25-mediated ubiquitination and activation of RIG-I as a potential feedback inhibitory pathway (Inn et al., 2011). These findings indicate that LUBAC plays important roles in various surface and intracellular PPR pathways as a positive and negative factor.

The inflammasome family of PRRs detects cytosolic pathogens and danger signals, such as potassium efflux and mitochondrial damage, in myeloid-lineage cells and responds by forming an oligomer signaling complex that includes an adapter protein, such as ASC or Naip5, which can bind to pro–caspase-1 (Franchi et al., 2012). The inflammasome complex subsequently potentiates the autocatalytic cleavage of pro–caspase-1 to its active p10 and p20 subunits, which enzymatically cleaves pro–IL-1β and pro–IL-18 to active cytokines for immediate secretion and inflammatory action (Schroder and Tschopp, 2010). Expression of the *pro–IL-1β* gene is NF-κB–dependent, and is triggered by a second PRR stimulation, such as TLRs, in macrophage cells (Schroder and Tschopp, 2010; Franchi et al., 2012). Regulation of inflammasomes by ubiquitination has previously been shown for the NLRP3 and AIM2 inflammasomes, which both use the ASC adapter protein (Franchi et al., 2012). The deubiquitination of NLRP3 by the BRCC3 complex is required for NLRP3 activation (Juliana et al., 2012; Lopez-Castejon et al., 2013; Py et al., 2013), and the K63-linked ubiquitination of ASC targets the AIM2–ASC inflammasome complex for destruction in autophagosomes (Shi et al., 2012; Shimada et al., 2012). However, given the complexity of the regulation of the NF-κB pathway by a combination of K63, K48, and linear ubiquitination, further analysis of ubiquitination-mediated regulation is necessary to fully understand inflammasome-induced innate immune pathways.

Besides its role in TLR-induced NF-κB activation, LUBAC-mediated linear ubiquitination may also participate in the inflammasome activation pathway for caspase-1 activation and IL-1β secretion. However, the roles of LUBAC have so far been defined through the study of mouse embryonic fibroblasts (MEFs), B cells and keratinocytes of HOIL-1L$^{-/-}$ and Sharpin^{cpdm} (null point mutant) mice, or human embryonic kidney (HEK293T) reporter cells with gene overexpression of knockdown conditions (Tokunaga et al., 2009, 2011; Gerlach et al., 2011; Ikeda et al., 2011) that do not express all of the subunits of the inflammasome family of PRRs, thus making the role of LUBAC in inflammasome pathways elusive. In this study, we thus examined the role of the HOIL-1L subunit of LUBAC in NLRP3 inflammasome pathway in primary BM-derived macrophages (BMDMs). We demonstrate that HOIL-1L is essential for NLRP3 inflammasome activation independently of NF-κB activation. Specifically, HOIL-1L is required for ASC linear ubiquitination and NLRP3 inflammasome assembly, thus expanding the role of LUBAC as an innate immune regulator.

RESULTS

Cell type–specific roles of HOIL-1L in NF-κB activation

To test whether NF-κB is regulated by LUBAC in macrophage cells, we first examined NF-κB activation in WT and HOIL-1L$^{-/-}$ BMDMs and MEFs upon stimulation with LPS or TNF (Fig. 1). Similarly to previous studies (Tokunaga et al., 2009, 2011; Gerlach et al., 2011; Ikeda et al., 2011), HOIL-1L$^{-/-}$ MEFs showed delayed kinetics of IκBα degradation compared with WT MEFs upon LPS or TNF treatment. In distinct contrast, HOIL-1L$^{-/-}$ BMDMs had similar kinetics of IκBα degradation to WT BMDMs (Fig. 1 a), suggesting that HOIL-1L may function in a cell type–dependent manner as previously shown in human patient samples (Boisson et al., 2012). As a result of reduced NF-κB activation, HOIL-1L$^{-/-}$ MEFs had reduced expression of the *IL-6*, *IκBα*, and *ICAM1* genes as compared with WT MEFs after 2 h of LPS treatment (Fig. 1 b). The relative abundances of *IL-6* transcripts in BMDMs and MEFs resulted in similar levels of IL-6 cytokine secretion in WT and HOIL-1L$^{-/-}$ BMDMs but significantly reduced IL-6 cytokine secretion in HOIL-1L$^{-/-}$ MEFs compared with WT MEFs after 24 h of LPS stimulation (Fig. 1 c), suggesting that HOIL-1L has cell type–specific functions for NF-κB activation.

To further define the role of HOIL-1L in NF-κB–dependent and –independent gene expression, we examined global mRNA transcripts by microarray and found that HOIL-1L$^{-/-}$ BMDMs had generally similar transcriptional profiles to WT BMDMs with or without LPS or TNF treatment (4 h;

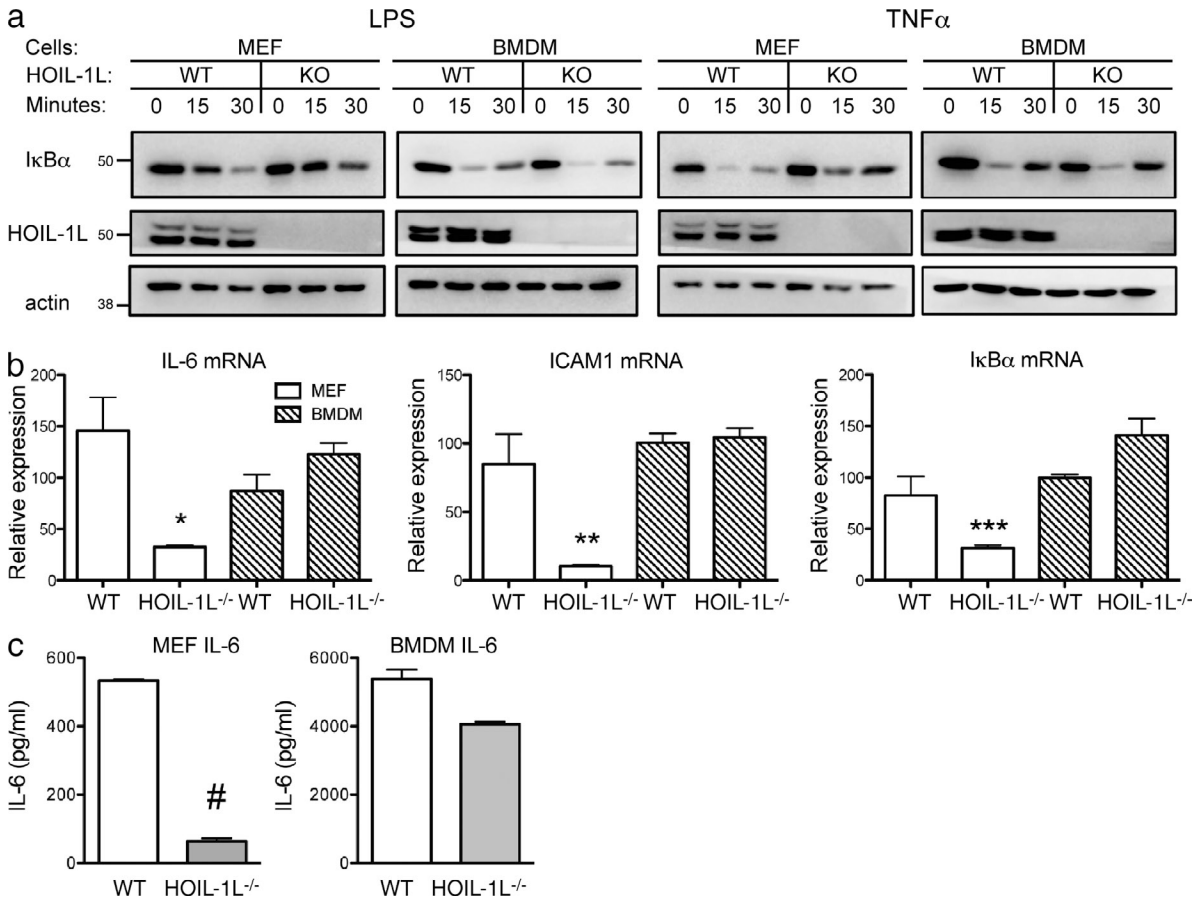

Figure 1. HOIL-1L has cell type–specific roles in NF-κB activation. (a) WT and HOIL-1L$^{-/-}$ MEFs and BMDMs were stimulated with 1 ng/ml TNF or 10 ng/ml LPS for 0, 15, or 30 min and probed for indicated protein levels by immunoblotting. Data are representative of three independent experiments. (b) The mRNA transcript abundance for selected NF-κB–regulated genes was quantified after 2 h of 10 ng/ml LPS stimulation by qRT-PCR (biological $n = 2$). Data are representative of two independent experiments. (c) IL-6 secretion was quantified by ELISA at 24 h after LPS treatment (biological $n = 3$). Data are representative of three independent experiments. Protein size markers are indicated in kD. All data are presented as the mean ± SEM by a Student's *t* test. *, P = 0.013; **, P = 0.015; ***, P = 0.034; #, P = 10^{-6}.

Fig. 2 a), whereas a small number of transcripts were differentially regulated in HOIL-1L$^{-/-}$ BMDMs compared with WT BMDMs (Tables S1 and S2). These transcripts might be directly regulated by HOIL-1L because HOIL-1L was originally identified as a DNA-binding protein, although the transcripts regulated by HOIL-1L were not previously identified (Tatematsu et al., 1998; Tokunaga et al., 1998). Specific comparison of the selected NF-κB–regulated transcripts further revealed equivalent or higher levels of their expression in HOIL-1L$^{-/-}$ BMDMs than in WT BMDMs, and pathway analysis confirmed that the NF-κB pathway was regulated in a similar manner in WT and HOIL-1L$^{-/-}$ BMDMs (Fig. 2 b). These expression profiles were additionally confirmed by quantitative PCR (qPCR) in WT and HOIL-1L$^{-/-}$ BMDM (Fig. 2 c). Notably, IL-1β transcript levels were similar in HOIL-1L$^{-/-}$ and WT BMDMs upon LPS treatment, confirming that LPS treatment is a suitable priming signal for inflammasome activation experiments in these cells. Previous microarray data of TLR2-activated WT and Sharpin^{cpdm} BMDMs showed an obvious defect in NF-κB–dependent gene expression (Zak et al., 2011), including a strong reduction of IL-1β transcript levels in Sharpin^{cpdm} BMDMs (Zak et al., 2011). Therefore, we did not include these cells for further study of inflammasome activation.

HOIL-1L is required for ASC-dependent inflammasome activation

To determine whether HOIL-1L is a regulator of inflammasome-mediated caspase-1 activation, WT and HOIL-1L$^{-/-}$ BMDMs were primed with LPS to induce the TLR4-dependent expression of pro–IL-1β protein, and subsequent activation of the NLRP3 inflammasome was achieved by treatment with nigericin, a potassium ionophore, silica particles, monosodium urate crystals (MSUs), or the peptidoglycan component MDP, followed by ATP treatment (Dostert et al., 2008; Hornung et al., 2008; Schroder and Tschopp, 2010; Kovarova et al., 2012). The AIM2 inflammasome was stimulated by double-stranded plasmid DNA (dsDNA) and the NLCR4 inflammasome was stimulated by cytosolic delivery of purified *Salmonella typhimurium*–derived flagellin or infection

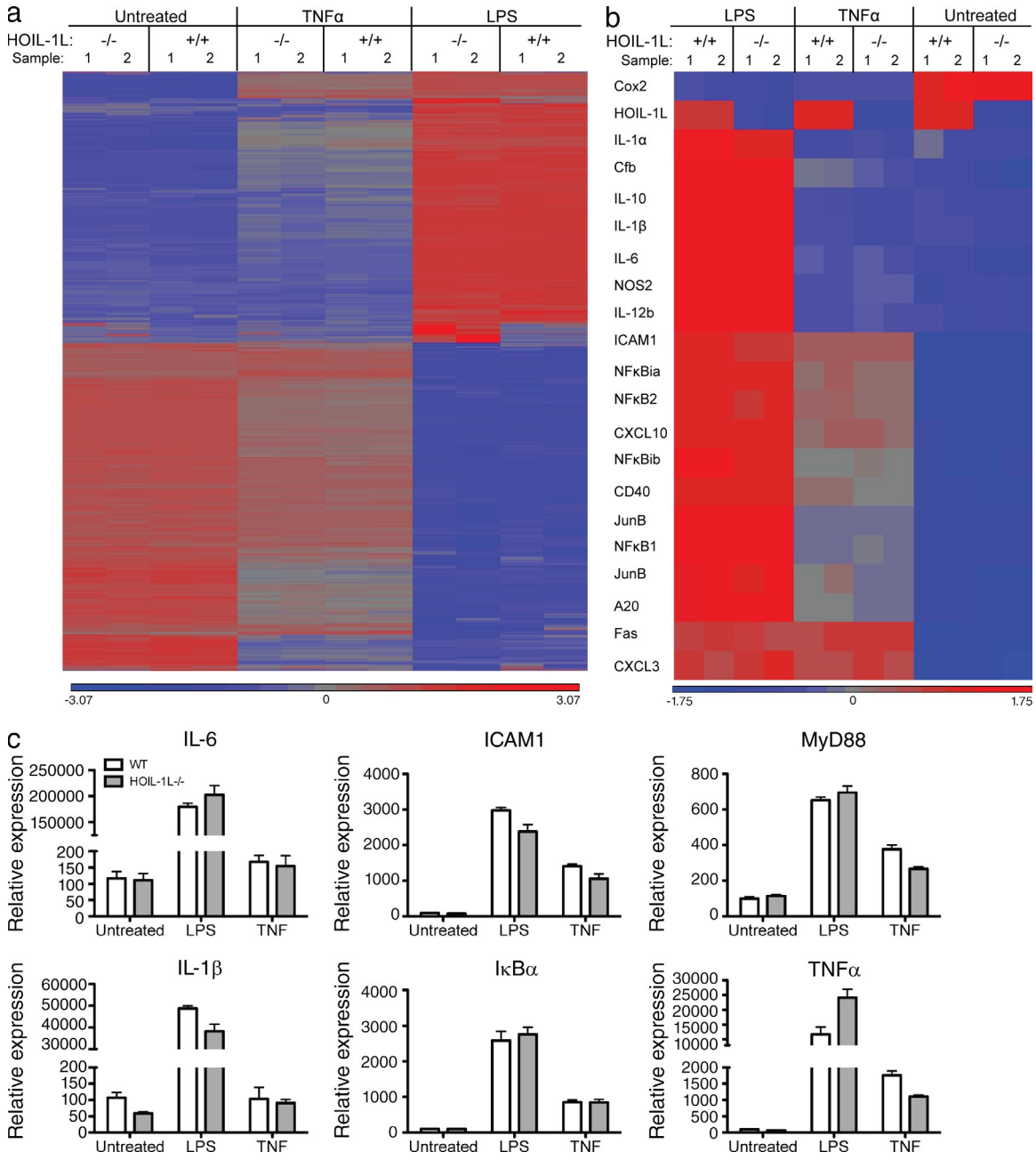

Figure 2. Global transcriptional profiles of WT and HOIL-1L$^{-/-}$ BMDMs in response to LPS and TNF. (a) Heat map of genes with fivefold or greater changes in expression by whole genome microarray comparison were grouped by hierarchal clustering for WT and HOIL-1L$^{-/-}$ BMDMs treated with 1 ng/ml TNF for 4 h, 10 ng/ml LPS for 4 h, or untreated for 4 h (biological $n = 2$, data for both individual replicates are presented as samples 1 and 2 for each condition). (b) Heat map of selected NF-κB genes compared by hierarchal clustering (biological $n = 2$, data for both individual replicates are presented as samples 1 and 2 for each condition). (c) Analysis of mRNA transcript abundance by qRT-PCR for selected genes as indicated in WT and HOIL-1L$^{-/-}$ BMDMs stimulated as in a (biological $n = 2$ and analytical $n = 2$ for each biological replicate). All data are presented as the mean ± SEM by a Student's t test.

with *Legionella pneumophila* without any additional priming. Compared with WT BMDMs, HOIL-1L$^{-/-}$ BMDMs had a defect in mature IL-1β secretion upon NLRP3 stimulation, reduced IL-1β secretion upon AIM2 stimulation, but similar IL-1β secretion upon NLRC4 stimulation (Fig. 3 a). Interestingly, the AIM2 (Fernandes-Alnemri et al., 2009; Rathinam et al., 2010) and NLRP3 (Martinon et al., 2002; Pan et al., 2007; Franchi et al., 2012) inflammasomes both require the adapter protein ASC, whereas the NLRC4 inflammasome is only enhanced by ASC (Broz et al., 2010; Miao et al., 2010; Zhao et al., 2011). Thus, these results indicate that HOIL-1L may specifically be required for ASC-dependent inflammasome activation. Although the IL-1β secretion induced by both NLRP3 and AIM2 inflammasomes were affected in HOIL-1L$^{-/-}$

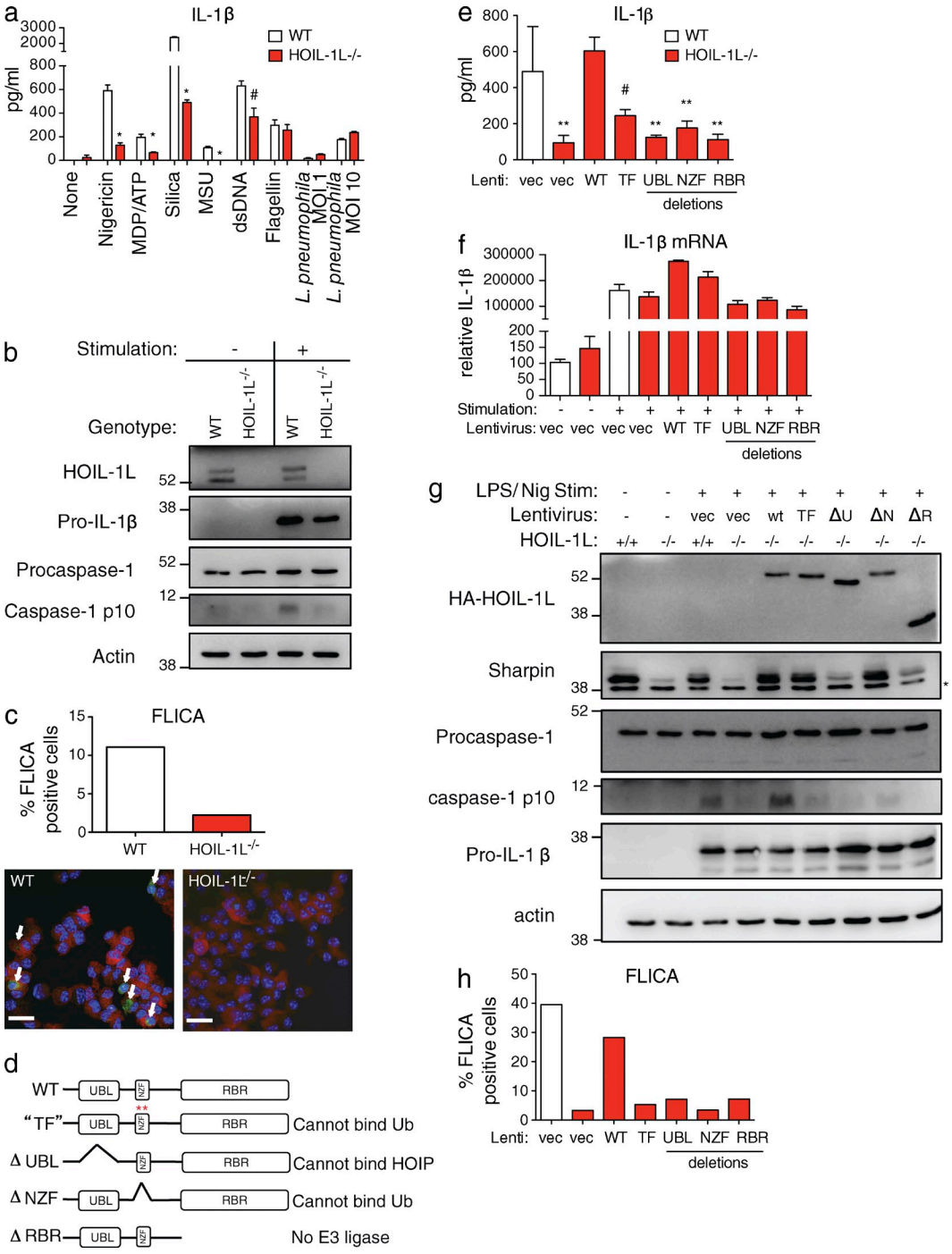

Figure 3. LUBAC is required for NLRP3 inflammasome activation in BMDMs. (a) IL-1β secretion as determined by ELISA of WT or HOIL-1L$^{-/-}$ BMDMs primed with LPS overnight and stimulated with nigericin, silica, MSU, MDP followed by ATP, dsDNA transfected by lipofectamine, or infected with adenovirus-Flagellin as indicated. Unprimed BMDMs were infected with *L. pneumophila* at indicated multiplicities of infection (MOIs). Data are presented as the mean ± SEM by a Student's *t* test (biological $n = 3$ and are representative of two independent experiments; *, $P < 0.00033$; #, $P = 0.011$). (b) Protein expression and caspase-1 cleavage of WT or HOIL-1L$^{-/-}$ BMDMs untreated or primed with LPS and stimulated with nigericin was analyzed by immunoblotting. (c) BMDMs primed with LPS and stimulated with nigericin were treated with FAM-YVAD-FLICA fluorescent caspase-1 substrate during MDP treatment, fixed, and then stained for caspase-1. The percentage of FLICA-positive cells was determined for 250 total cells. Arrows point to FLICA-stained spots. Bars, 20 µm. (d–h) WT or HOIL-1L$^{-/-}$ BMDMs were complemented with lentiviral vectors expressing mutants described in d and analyzed for: (e) IL-1β secretion by ELISA (biological $n = 3$ and analytical $n = 2$; data presented as the mean ± SEM; **, $P < 0.0075$; #, $P < 0.013$ by a Student's *t* test); (f) mRNA quantification by qRT-PCR; (g) protein expression by immunoblot; and (h) quantification of FLICA staining for active caspase-1. All data are representative of three independent experiments except for c and h, which depict combined data for all three experiments. Protein size markers are indicated in kD.

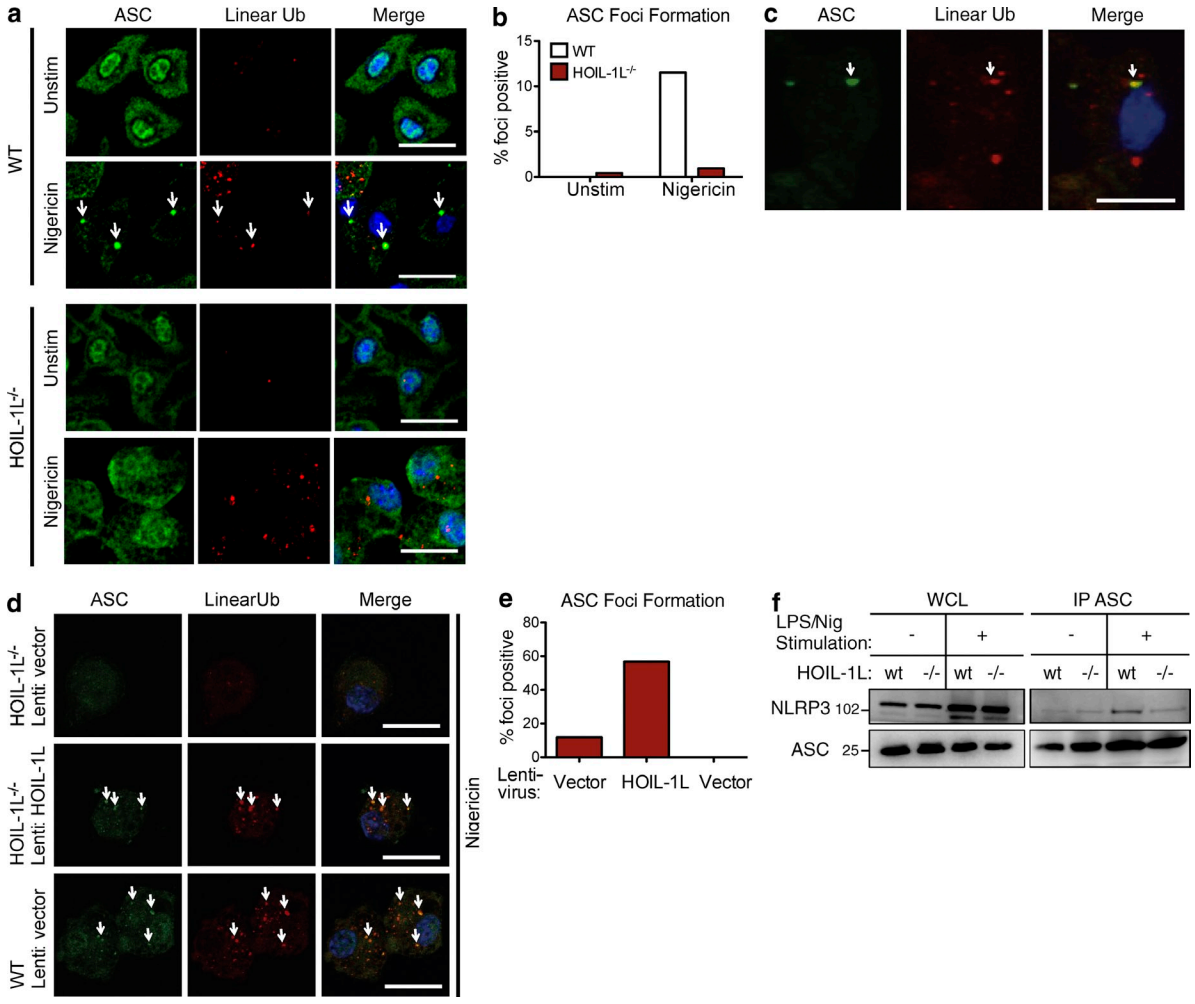

Figure 4. Assembly of the NLRP3/ASC inflammasome requires HOIL-1L. (a) Representative images of ASC foci formation (arrows) upon NLRP3 stimulation in WT or HOIL-1L$^{-/-}$ BMDMs with ASC staining in green, linear ubiquitin in red, and nuclei in blue. Bar, 20 µm. Images are from one of four independent experiments. (b) Quantification of ASC foci in 100 cells counted from images in a. (c) Z-stack of WT BMDMs in a. Bar, 10 µm. (d) Representative images of ASC foci formation (arrows) upon NLPR3 stimulation in HOIL-1L$^{-/-}$ and WT BMDMs infected with indicated lentiviruses and stained as described for a. Bar, 20 µm. Images are from one of two independent experiments. (e) Quantification of ASC foci from 30 cells combined from three experiments from images in d. (f) IP of ASC from untreated WT and HOIL-1L$^{-/-}$ BMDMs or after LPS priming and nigericin stimulation, data are representative of four independent experiments. Protein size markers are indicated in kD.

BMDMs, the effect was much more pronounced for NLRP3 stimulation than for AIM2 stimulation, leading us to further characterize the mechanism of HOIL-1L–mediated regulation of NLRP3–ASC inflammasome activation. Although WT BMDMs had NLRP3 stimulation-dependent caspase-1 activity, as measured by pro–caspase-1 cleavage to the p10 subunit, HOIL-1L$^{-/-}$ BMDMs showed a defect in pro–caspase-1 cleavage under the same stimulation conditions (Fig. 3 b). Similarly, when BMDMs were stained with FAM-YVAD-FMK (FLICA), a fluorescent caspase-1 substrate peptide which selectively binds cleaved and active caspase-1 enzyme, only WT BMDMs contained FLICA-staining positive active caspase-1 upon NLRP3 stimulation, whereas HOIL-1L$^{-/-}$ BMDMs had reduced FLICA staining (Fig. 3 c). Together, these data demonstrate that LUBAC is a critical regulator for the NLRP3 stimulation-dependent activation of caspase-1 activity.

To define the role of linear ubiquitination in inflammasome activation, we complemented the HOIL-1L$^{-/-}$ BMDMs with HA-tagged WT or mutant HOIL-1L (Fig. 3 d). These mutants are as follows: the ΔUBL mutant carrying deletion of the ubiquitin-like (UBL) domain that is required for binding to HOIP to achieve linear ubiquitination activity (Kirisako et al., 2006; Stieglitz et al., 2012); the ΔNZF and TF mutants carrying deletion and T203L/F204V point mutations, respectively, of the Npl4 type-zinc-finger (NZF) domain that is required for binding to ubiquitin (Haas et al., 2009; Sato et al., 2011); and the ΔRBR mutant carrying deletion of the Ring-between-Ring (RBR) domain that is an E3 ubiquitin ligase domain. As expected, pro–IL-1β mRNA and

protein levels were not affected by WT or mutant HOIL-1L gene expression (Fig. 3, f and g). Complementation of HOIL-1L$^{-/-}$ BMDMs with WT HOIL-1L fully rescued pro–caspase-1 cleavage, caspase-1 activity, and IL-1β secretion (Fig. 3, e–h). However, deletion of the UBL, NZF, or RBR domain of HOIL-1L failed to restore pro–caspase-1 cleavage, caspase-1 activity, or IL-1β secretion (Fig. 3, e–h). Together, these data indicate that nearly all the functional components of HOIL-1L, including the N-terminal HOIP interaction, the central ubiquitin interaction, and the C-terminal ubiquitination ligase activity, are critical for pro–caspase-1 cleavage and enzymatic activity in NLRP3-inflammasome activation.

HOIL-1L is required for NLRP3/ASC inflammasome assembly

We next examined whether linear ubiquitination was important for inflammasome activation events occurring upstream of caspase-1 cleavage, namely, ASC cytoplasmic foci formation and NLRP3–ASC complex assembly. Similarly to previous reports (Bryan et al., 2009; Shi et al., 2012; Proell et al., 2013), ASC had diffuse localization in unstimulated WT BMDMs and could be found in distinct cytoplasmic foci upon NLRP3 stimulation (Fig. 4, a and b). Furthermore, when WT BMDMs were stained with a linear ubiquitin-specific antibody, ASC foci effectively colocalized with linear ubiquitination-containing compartments; Z-stack confocal imaging revealed that the linear ubiquitination-containing compartments appeared to be in the center of the ASC foci (Fig. 4 c and Video 1). Complementation of HOIL-1L$^{-/-}$ BMDMs with HOIL-1L fully rescued ASC foci formation and the colocalization of ASC foci with linear ubiquitin stains to nearly the same levels as WT BMDMs (Fig. 4, d and e). Although linear ubiquitination-containing compartments were detectable in HOIL-1L$^{-/-}$ BMDMs, they did not colocalize with the ASC that remained diffuse throughout the cytoplasm in either untreated or NLRP3-stimulation conditions (Fig. 4 a). Furthermore, immune purification showed the efficient formation of the NLRP3–ASC complex in LPS-primed, nigericin-stimulated WT BMDMs (Fig. 4 f). By marked contrast, the formation of the NLRP3–ASC complex was reduced to background levels in HOIL-1L$^{-/-}$ BMDMs under the same conditions (Fig. 4 f). These results indicate a critical role of LUBAC in ASC foci formation and NLRP3–ASC inflammasome assembly.

ASC is linear ubiquitinated by LUBAC

Because ASC foci colocalized with linear ubiquitin-containing compartments in WT BMDMs upon NLRP3 stimulation, we evaluated by five different assays whether ASC is a potential LUBAC substrate. First, we used a linear ubiquitin-specific antibody to immunoprecipitate linear ubiquitin from 293 T cells transfected with the LUBAC subunits HOIL-1L and HOIP, along with a C-terminal Flag-tagged ASC (ASC-Flag) in 5M urea denaturation buffer conditions as optimized (Fig. S1) and as previously described (Matsumoto et al., 2012). Linear ubiquitin-specific immunoblotting indicated that high levels of linear ubiquitinated proteins were produced upon LUBAC expression (Fig. 5 a) and that ASC was detected as multi-laddered and high molecular weight bands in the linear ubiquitin immunoprecipitations (IPs), suggesting that ASC is a LUBAC substrate (Fig. 5 a). In addition, NEMO was also detected in the linear ubiquitin IP (Fig. S1) consistent with previous results (Tokunaga et al., 2009), whereas AIM2 and NLRP3 showed no linear ubiquitination (Fig. 5 a), demonstrating the substrate selectivity of LUBAC-mediated linear ubiquitination in 293T cells. Comparison of the E3-ligase activity in cells co-expressing different combinations of the WT or E3 ligase-defective "cs" mutants of HOIP and HOIL-1L—which have cysteine to serine point mutations at conserved residues of the RING domains in the C-terminal RBR region (Kirisako et al., 2006; Inn et al., 2011; Stieglitz et al., 2012)—revealed that the E3 ligase activities of both HOIP and HOIL-1L were required for the efficient linear ubiquitination of ASC. Specifically, expression of the HOIL-1L cs mutant markedly reduced levels of ASC linear ubiquitination, and expression of the HOIP cs mutant led to undetectable levels of ASC linear ubiquitination (Fig. 5 b). Linear ubiquitination does not appear to lead to the degradation of ASC by the proteasome because inhibition of the proteasome with MG132 did not affect levels of total or linear ubiquitinated ASC (Fig. 5 c). Consistently, endogenous ASC protein levels were comparable in WT and HOIL-1L$^{-/-}$ cell lysates (Fig. 4 f; and Fig. 6, a and b). These data are consistent with the presumed nondegradative effect of linear ubiquitination on the Nemo and Rip1 substrates (Iwai and Tokunaga, 2009; Tokunaga et al., 2009), and indicate that both the HOIP and HOIL-1L E3 ligase activities are required for the efficient linear ubiquitination of ASC.

In a second method for testing whether ASC is a LUBAC substrate, we purified linear ubiquitinated proteins from transfected 293T lysates with a bacterially produced GST fusion to the coiled zipper (CoZi) domain of NEMO that has been shown to specifically bind to both K63 and linear ubiquitin chains (Komander et al., 2009; Rahighi et al., 2009). In parallel, a GST-CoZi mutant fusion containing the R309A, R312A, E313A (rre) mutant, which cannot bind to linear ubiquitin chains but is capable of binding to K63-linked ubiquitin chains in vitro (Komander et al., 2009), was included as a control. Consistent with the linear ubiquitin IPs, the GST-CoZi purification pulled down ASC-Flag with multi-laddered high molecular weights in a LUBAC expression dependent manner, whereas the GST-CoZi rre mutant did not (Fig. 5 d), further supporting the LUBAC-mediated linear ubiquitination of ASC. Moreover, ASC linear ubiquitination was exclusively detected when HOIL-1L and HOIP were coexpressed, indicating that the linear ubiquitination of ASC is LUBAC-dependent (Fig. 5 d). In a third method, an in vitro ubiquitination assay also showed that HOIP-HOIL-1L co-purified from a bacterial expression system specifically ubiquitinated ASC-Flag protein to levels that were comparable to the previously identified Nemo substrate (Tokunaga et al., 2009; Fig. 5 e), indicating that the LUBAC, E1, and E2 enzymes are sufficient for the linear ubiquitination of ASC. When NLRP3-Flag was included as a control, no

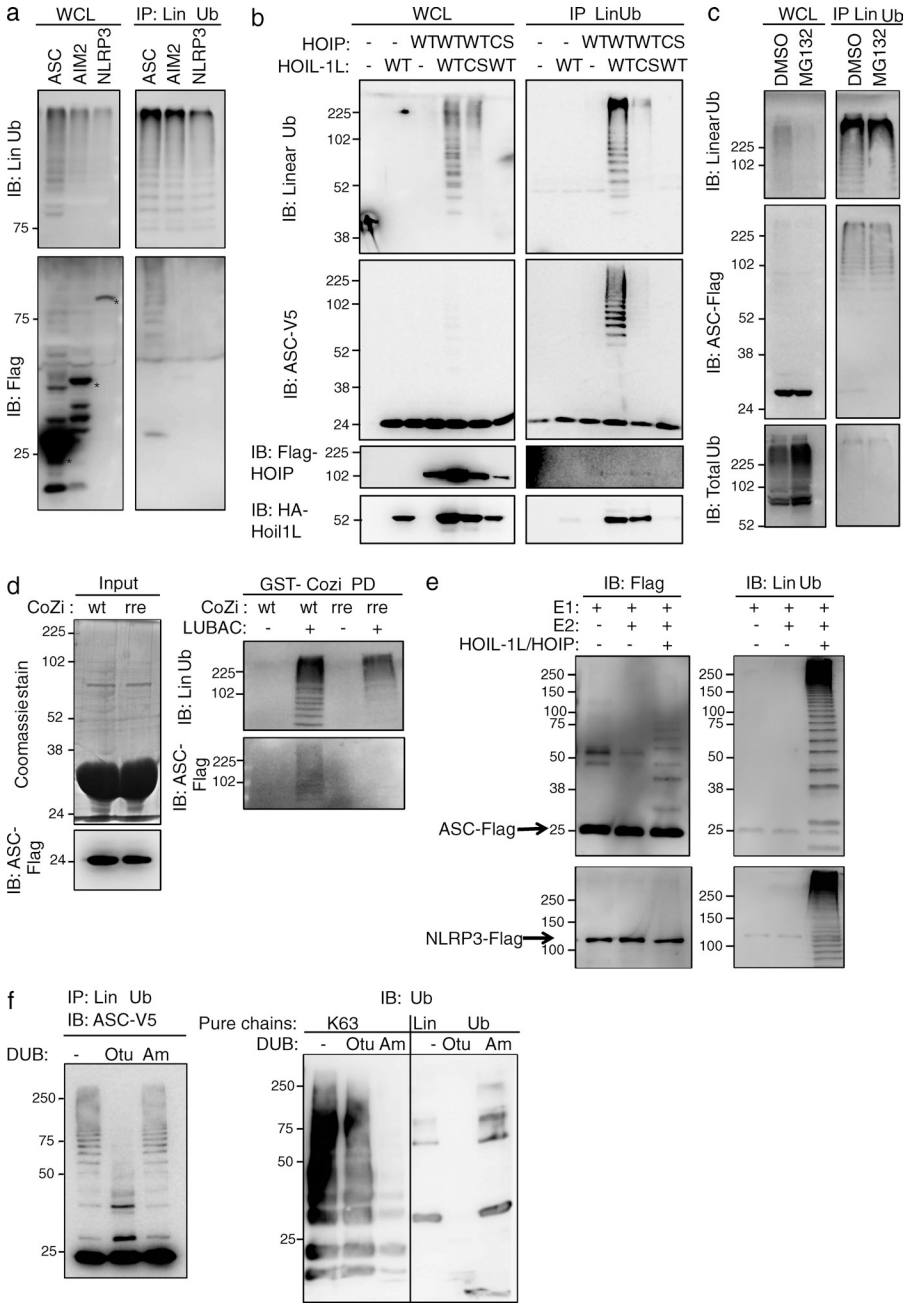

Figure 5. ASC is linear ubiquitinated by LUBAC in 293T cells and in vitro. (a) Flag-tagged ASC, AIM2, or NLRP3 were cotransfected with HOIL-1L-HA and myc-HOIP into 293T cells. Linear ubiquitinated proteins were immunoprecipitated. WCL (whole cell lysate) or immunoprecipitates (IP Lin Ub) were immunoblotted for Flag and linear ubiquitin. (b) 293T cells were transfected with a panel of WT HOIL-1L-HA and Flag-HOIP or RBR E3 ligase domain cysteine to serine point mutants (cs) and probed by linear ubiquitin IP for ASC-V5, HA, and Flag as indicated. (c) Transfected 293T cells were treated for 6 h with 20 µM MG132 or an equivalent volume of DMSO before lysates were collected and immunoprecipitated with linear ubiquitin antibody. Immunoprecipitates were probed for linear ubiquitin, Flag, and ubiquitin as indicated. (d) Bacterially purified GST-CoZi wt and rre proteins were incubated with lysates from 293T cells transfected with ASC-Flag, HOIL-1L-HA, and myc-HOIP or vector control plasmids (left, input). Proteins that were pulled down by WT or rre mutant GST-CoZi were probed for linear ubiquitin or Flag by immunoblotting (right, GST-Cozi PD). (e) ASC-Flag and NLRP3-Flag were purified from 293T lysates in a nondenaturing high salt buffer (500 mM NaCl) and combined as indicated with E1 (Ube1), E2 (UbcH5c), and LUBAC (HOIL-1L/HOIP) purified from bacteria in a linear ubiquitination reaction that was incubated for 18 h at 37°C. Reactions were stopped by the addition of loading dye and immunoblotted for Flag. Membranes were then stripped and reprobed for linear ubiquitin. (f) Deubiquitinase treatment of linear ubiquitin immunoprecipitates from 293T cell lysates overexpressing HOIL-1L-HA, myc-HOIP, and ASC-V5. Reactions were immunoblotted for linear ubiquitin and V5. Control purified ubiquitin chains were incubated in parallel in deubiquitinase reactions that were immunoblotted with a linkage nonspecific antibody against ubiquitin (Ub). All data are representative of a minimum of three independent experiments. * indicates unmodified size. Protein size markers are indicated in kD.

detectable in vitro linear ubiquitination of NLRP3 was observed under the same conditions (Fig. 5 e). In a fourth assay, linear ubiquitin immunoprecipitates were treated with the linear linkage-specific deubiquitinase Otulin, or the K63 linkage-specific deubiquitinase AMSH, to determine whether the ubiquitin chains on ASC were simply linear linkage or a mixture of K63 and linear linkages, which has previously been reported for other LUBAC substrates (Emmerich et al., 2013). Only the Otulin treatment reduced high molecular weight ASC, whereas the AMSH treatment had no effect (Fig. 5 f). Lastly, in a fifth assay, the linear ubiquitin IP of BMDM lysates indicated that overall linear ubiquitin levels increased in WT BMDMs upon NLRP3 stimulation but were reduced in HOIL-1L$^{-/-}$ BMDMs, whereas total ubiquitin levels remained the same (Fig. 6, a–d). Linear ubiquitin IP from WT BMDMs in 5M urea buffer precipitated the high molecular weight ASC protein, which was enhanced by NLRP3 stimulation (Fig. 6 a), indicating that endogenous ASC is linear ubiquitinated. Furthermore, levels of total linear ubiquitin and the linear ubiquitinated ASC were considerably reduced in HOIL-1L$^{-/-}$ BMDMs under NLRP3 stimulation conditions when compared with those in WT BMDMs (Fig. 6 b). Collectively, these results demonstrate that ASC is a specific substrate of LUBAC in overexpression and endogenous conditions.

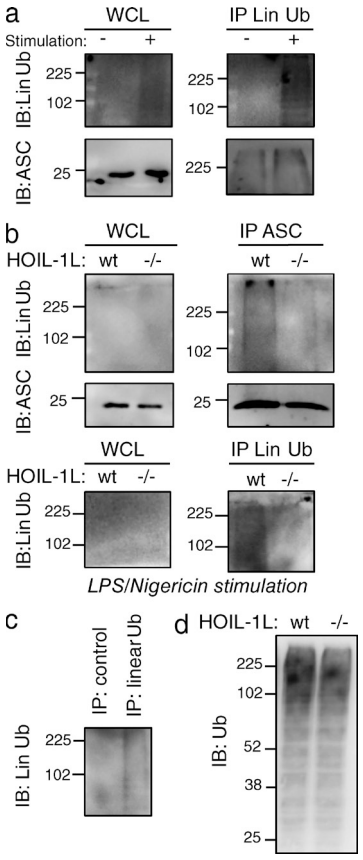

Figure 6. Endogenous mouse ASC is linear ubiquitinated in BMDMs. (a) WT BMDMs were untreated or primed with LPS overnight and stimulated with nigericin for 2 h before IP with a linear ubiquitin-specific antibody in 5M urea denaturing conditions. Immunoprecipitates (IP Lin Ub) and whole cell lysates (WCL) were immunoblotted for ASC and linear ubiquitin (Lin Ub). (b) WT and HOIL-1L$^{-/-}$ BMDMs were primed with LPS overnight and stimulated with nigericin for 2 h before IP with an ASC-specific antibody and extensive washing in high salt buffer (500 mM NaCl). Immunoprecipitates and WCLs were immunoblotted for ASC and linear ubiquitin. (c) WT BMDMs were primed with LPS overnight and stimulated with nigericin for 2 h before IP with a linear ubiquitin-specific antibody or an equivalent amount of control human antibody in 5M urea denaturing conditions. Immunoprecipitates and WCL were immunoblotted for linear ubiquitin. (d) WCL extracts from lysates in c were immunoblotted for ubiquitin with a linkage nonspecific antibody (Ub). All data are representative of two independent experiments. Protein size markers are indicated in kD.

Role of HOIL-1L in NLRP3-induced IL-1β production and inflammation in vivo

Previous reports of the MDP-induced peritonitis mouse model (Bruey et al., 2007; Pan et al., 2007; Shenoy et al., 2012) have demonstrated that NOD2, a cytosolic PRR in the NLR family, is required for NF-κB–mediated IL-6 production, whereas NLRP3 is required for IL-1β secretion and neutrophil recruitment in i.p. cavity. Thus, we tested whether HOIL-1L was important for proinflammatory cytokine production and neutrophil recruitment in the MDP-induced peritonitis mouse model. As expected, WT mice had increased IL-6 and IL-1β production and neutrophil recruitment to the IP cavity after injection with MDP (Fig. 7). Interestingly, IL-1β production and neutrophil recruitment were significantly reduced in HOIL-1L$^{-/-}$ mice compared with WT mice, whereas IL-6 production was similar in WT and HOIL-1L$^{-/-}$ mice (Fig. 7). These results suggest that HOIL-1L is required for NLRP3-dependent IL-1β production and neutrophil recruitment, but not for NOD2-dependent IL-6 production, in MDP-induced peritonitis in vivo.

We also examined the role of HOIL-1L in an LPS-induced systemic inflammation mouse model in vivo, which is dependent on several inflammatory signaling molecules including TLR4, NLRP3, ASC, and IL-1β (McNamara et al., 1993; Mariathasan et al., 2004, 2006; Joosten et al., 2010; Kayagaki et al., 2013). The WT control mice rapidly succumbed to LPS challenge beginning at 24 h after injection and continuing until 72 h after injection. The WT mice also showed high levels of inflammation as measured by hematoxylin, eosin, and apoptotic marker Annexin V staining of spleen sections at 24 h after injection (Fig. 8, a and b), indicating that excessive inflammation contributed to the deaths of the WT mice. In contrast, 100% of the HOIL-1L$^{-/-}$ mice survived LPS challenge despite significant weight loss (Fig. 8, a and c). HOIL-1L$^{-/-}$ mice also had significantly lower serum IL-1β levels and Annexin-V staining of splenic sections at 24 h after injection (Fig. 8, b and d), suggesting the HOIL-1L$^{-/-}$ mice had reduced inflammatory responses. Because NLRP3$^{-/-}$ and ASC$^{-/-}$ mice are also resistant to LPS in this mouse model (Mariathasan et al., 2004, 2006), the role of HOIL-1L in NLRP3 inflammasome activation characterized here may also contribute to the survival of HOIL-1L$^{-/-}$ mice in the LPS-induced lethal inflammation model in vivo.

DISCUSSION

Here, we demonstrate that HOIL-1L is specifically required for NLRP3 inflammasome-dependent IL-1β secretion in BMDMs independently of NF-κB activation. Mechanistically, the assembly of the NLRP3/ASC inflammasome and linear ubiquitination of the novel LUBAC substrate, ASC, both require HOIL-1L expression. The loss of these functions in HOIL-1L$^{-/-}$ mice results in resistance to MDP-induced peritonitis and contributes to survival upon LPS-induced systemic inflammation. This is the first demonstration that linear ubiquitination is required for NLRP3/ASC-dependent inflammasome activation, thus expanding the role of LUBAC as an innate immune regulator. This work is also the first to compare the role of HOIL-1L in MEF and macrophage cells. Our data indicate that HOIL-1L is critical for NF-κB activation in MEF cells, consistent with the literature (Fig. 1; Tokunaga et al., 2009; Gerlach et al., 2011; Ikeda et al., 2011). However, this activity is cell type specific because HOIL-1L is not required for NF-κB activation or NF-κB–dependent gene expression in BMDMs (Figs. 1 and 2). These observations are likely clinically relevant because patients lacking functional HOIL-1L expression had an IL-6 response to LPS that was equivalent to control patient levels when whole blood cells were stimulated (Boisson et al., 2012), which is

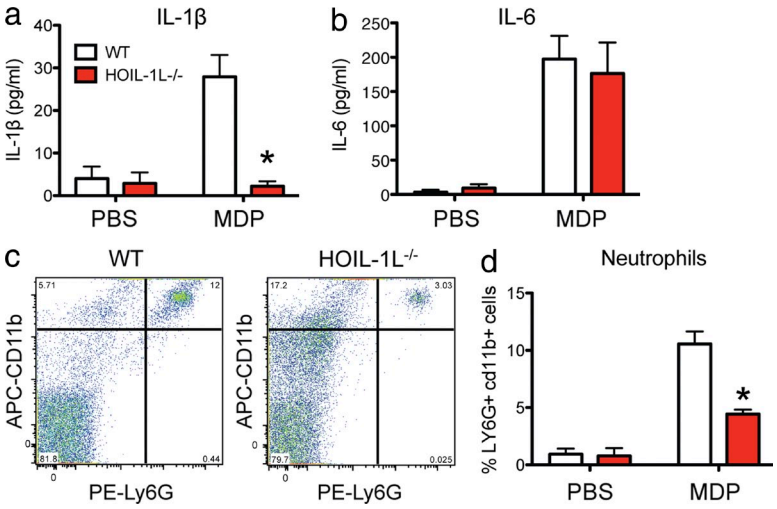

Figure 7. HOIL-1L is required for MDP-induced peritonitis in vivo. WT and HOIL-1L$^{-/-}$ mice were injected i.p. with PBS or MDP to induce peritonitis. 5 h later, IP wash fluid was analyzed for IL-1β (a) and IL-6 (b) levels by ELISA and infiltrating Ly6G/CD11b double-positive neutrophils (c and d) were quantified by flow cytometry (biological $n = 8$ from three independent experiments). All data are presented as the mean ± SEM. *, P < 0.00015 by a Student's *t* test.

similar to our results in BMDMs (Fig. 2, b and c). However, IL-6 production was attenuated in fibroblast cells of HOIL-1L–deficient patients (Boisson et al., 2012) similarly to our results with HOIL-1L$^{-/-}$ MEFs (Fig. 1 c), indicating that the tissue-specific functions for HOIL-1L also exist in humans. Because HOIL-1L–deficient patients were prone to pyogenic bacterial infections (Boisson et al., 2012), we predict that a defect likely exists in NLRP3 inflammasome assembly in these patients, similar to what we have observed in BMDMs from HOIL-1L$^{-/-}$ mice, leading to ineffective innate immunity upon exposure to bacterial pathogens. In addition to cell type–specific functions for HOIL-1L, the LUBAC subunit Sharpin may also have tissue-specific roles. It has been reported that Sharpin^{cpdm} MEFs (Gerlach et al., 2011; Ikeda et al., 2011; Tokunaga et al., 2011) and BMDMs (Zak et al., 2011) have defects in NF-κB signaling, yet skin cells from Sharpin^{cpdm} mice have elevated NF-κB activation (Liang, 2011; Liang et al., 2011), suggesting that Sharpin has unique functions in skin cells. In fact, the dermatitis phenotype observed in Sharpin^{cpdm} mice is reversed by NF-κB inhibitor treatment (Liang et al., 2011) or knockout of the TNF gene (Gerlach et al., 2011), further supporting cell type–dependent roles for Sharpin.

Our microarray data results indicated that expression of several genes was up-regulated in HOIL-1L$^{-/-}$ BMDM relative to WT BMDM in response to LPS and TNF stimulation (Fig. 2 a and Table S2), suggesting that HOIL-1L is perhaps a negative regulator of LPS- and TNF-mediated signaling in BMDMs. It is possible that our list of genes for which transcription levels are significantly different in HOIL-1L$^{-/-}$ BMDMs compared with WT BMDMs includes those that HOIL-1L may directly regulate as a potential transcription factor (Tatematsu et al., 1998; Tokunaga et al., 1998; Tables S1 and S2). However, the majority of genes in the list are uncharacterized, making the relevance of HOIL-1L–mediated regulation of their gene expression unclear. A previous microarray compared WT and Sharpin^{cpdm} BMDMs upon stimulation of

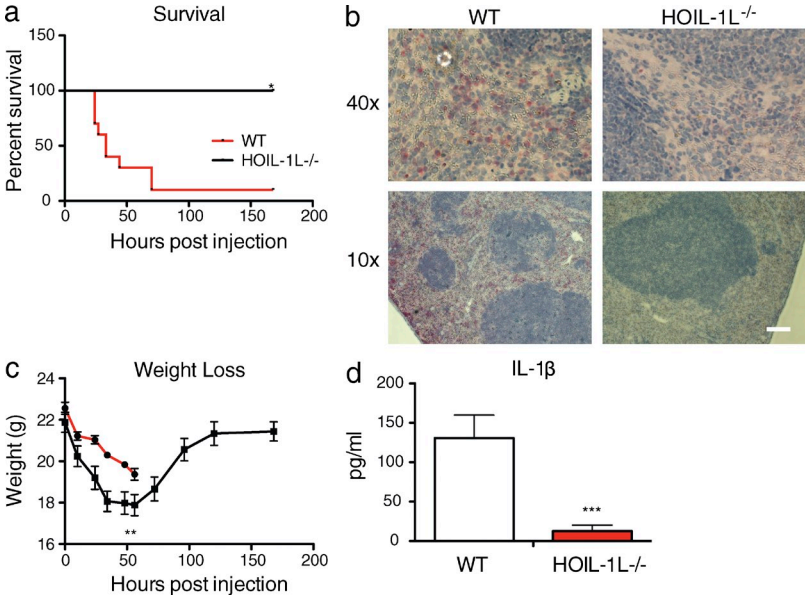

Figure 8. HOIL-1L is required for lethal inflammation upon LPS challenge in vivo. (a) Survival curve for WT or HOIL-1L$^{-/-}$ mice challenged with 30 mg/kg LPS ($n = 10$, combined from three independent experiments). (b) Apoptotic marker Annexin-V (red) and hematoxylin-eosin (H&E)–stained spleen sections from mice in a, sacrificed 24 h after LPS injection. Images are representative of three analyzed mice for each condition. Bar, 100 µm. (c) Weight curve of mice from a. (d) Serum IL-1β levels from WT and HOIL-1L$^{-/-}$ mice sacrificed 24 h after LPS injection were determined by ELISA ($n = 4$, combined from 2 independent experiments). Data are presented as the mean ± SEM. *, P < 0.0001 by a Log-rank Mantel-Cox test; **, P = 0.0015; ***, P < 0.008 by a Student's *t* test.

TLR2 with bacterial lipoprotein Pam3CSK4 and found a significant defect in NF-κB–dependent transcription in Sharpin^{cpdm} BMDMs (Zak et al., 2011). Because HOIL-1L$^{-/-}$ mice do not exhibit the severe dermatitis phenotypes of the Sharpin^{cpdm} mice (Gerlach et al., 2011; Ikeda et al., 2011), it is not surprising to find that these LUBAC members have different roles in various signaling pathways. In contrast to our observation that IL-6 secretion is not impaired in HOIL-1L$^{-/-}$ mice in response to MDP (Fig. 7), a previous study reported that Sharpin^{cpdm} BMDMs have a defect in MDP-dependent IL-6 secretion, although an in vivo peritonitis model was not used in this study (Damgaard et al., 2012). This difference could also be due to the use of lipid modified MDP (L18-MDP) in the previous study, or it could indicate that HOIL-1L and Sharpin may have different roles in NOD2 stimulation. Additional reports that LUBAC is recruited to the NOD2 receptor complex in response to MDP suggest that this recruitment requires XIAP. However, the role of LUBAC was not directly tested in these studies. In addition, the defects in XIAP-deficient cells and Otulin-expressing cells could be due to LUBAC-independent functions of XIAP or difference of nonmacrophage cell types used in these studies (Damgaard et al., 2013; Keusekotten et al., 2013). Further study is necessary to resolve the detailed roles of LUBAC in gene expression regulation.

Ubiquitination is a posttranslational modification that creates versatility in intracellular signaling. Specifically, K63 linkage is exclusively responsible for ubiquitin-mediated nondegradative signaling functions and linear linkage is crucial in various receptor and PRR pathways. Our discovery of ASC as a LUBAC substrate is related to a previous report that ASC is ubiquitinated upon AIM2 stimulation (Shi et al., 2012), although K63-linked ubiquitination was reported. Because K63 antibodies can cross-detect linear ubiquitination (Matsumoto et al., 2012) and the K63 E3 ligase or ASC lysine targets were not identified, it may be possible that the ubiquitination in this previous study was actually linear ubiquitination. Ubiquitination of NLRP3 has also been reported (Lopez-Castejon et al., 2013; Py et al., 2013); however, this ubiquitination is not likely to be linear because the N-terminal His-tagging of ubiquitin used in this study would eliminate the possibility of a linear methionine-to-glycine linkage (Gerlach et al., 2011). Previous characterization of Nemo as a LUBAC substrate used 293T overexpression systems, reporter assays, and in vitro assays (Tokunaga et al., 2009, 2011; Gerlach et al., 2011; Ikeda et al., 2011). Our results demonstrate that ASC is a LUBAC substrate using similar assays, with additional endogenous evidence in BMDMs (Figs. 5 and 6). Previous mapping of the Nemo protein led to the identification of two lysine targets for LUBAC, which were functionally required for NF-κB activation in MEF cells (Tokunaga et al., 2009). We also expect that two linear ubiquitination sites may exist on ASC based on the results from our deubiquitination assay (Fig. 5 f). Because Otulin can more efficiently cleave linear ubiquitin linkages than ubiquitin-substrate linkages, the two higher molecular weight ASC bands that remained after Otulin treatment (Fig. 5 f) may correspond to two direct ubiquitination sites on ASC. However, our attempts to map the ubiquitinated residues of ASC indicate that mutagenesis of the lysines in ASC affects protein–protein interactions independently of linear ubiquitination, making finer evaluation of the role of ASC linear ubiquitination for inflammasome activation difficult. Furthermore, as shown in the Nemo linear ubiquitination studies (Tokunaga et al., 2009, 2011; Gerlach et al., 2011; Ikeda et al., 2011), the levels of endogenous linear ubiquitination of Nemo seem to be very low. Thus, additional technical advances are necessary to define the specific roles of linear ubiquitination in intracellular signaling pathways.

Our data supports the hypothesis that each type of inflammasome has unique regulatory mechanisms, although the detailed mechanisms for these events have not been completely described. In particular, the NLRP3 inflammasome is distinct from other inflammasome sensors because it responds to a wide variety of triggers instead of one or two specific ligands like AIM2 or NLRC4 (Schroder and Tschopp, 2010; Franchi et al., 2012). Although mitochondrial damage is a common source for the potential NLRP3 stimulating signals, including mitochondrial ROS, oxidized mitochondrial DNA, and mitochondrial cardiolipin (Nakahira et al., 2011; Shimada et al., 2012; Iyer et al., 2013), the molecular events preceding the NLRP3/ASC interaction are not well characterized. Thus, it remains unknown what triggers HOIL-1L–containing LUBAC to linear ubiquitinated ASC upon NLRP3 stimulation. A recent report identified the phosphorylation of ASC as a trigger for the NLRP3 and AIM2 inflammasomes, although it is not clear whether this phosphorylation event affects the ubiquitination of ASC (Hara et al., 2013). Because the molecular events triggering caspase-1 cleavage are also unclear, the mechanisms of NLRP3 activation must be further defined to characterize which events happen first. Nevertheless, our work has added linear ubiquitination to the sequence of events that precede NLRP3/ASC inflammasome assembly.

The resistance of HOIL-1L$^{-/-}$ mice to lethal inflammation (Fig. 8) emphasizes the role of HOIL-1L as a critical regulator of inflammation in vivo despite the absence of dermatitis phenotype that is observed in the Sharpin^{cpdm} mice (Gerlach et al., 2011; Ikeda et al., 2011; Tokunaga et al., 2011). Given that the accurate mechanisms responsible for the symptoms of lethal inflammation in mouse models are not fully understood (Kayagaki et al., 2013; Seok et al., 2013), it is likely that HOIL-1L$^{-/-}$ mice are resistant to death because of complex multifaceted roles of HOIL-1L in inflammation, but not due to its action in a single pathway. Thus, the overall survival of the HOIL-1L$^{-/-}$ mice is likely due to a combination of various roles of HOIL-1L in different pathways, including NLRP3 activation, NF-κB–dependent TNF, IL-1β, CD40, and NOD2 receptor signaling (Haas et al., 2009; Iwai and Tokunaga, 2009; Tokunaga et al., 2009; Zak et al., 2011; Damgaard et al., 2012), protein kinase C activity (Nakamura et al., 2006), RIG-I activation (Inn et al., 2011), and transcriptional regulation as a DNA-binding protein (Tatematsu et al., 1998; Tokunaga et al., 1998). Interestingly, the HOIL-1L$^{-/-}$ mice never displayed any behavioral symptoms of LPS-induced lethal inflammation

(lethargy or shivering) even though they had considerably more weight loss as WT mice (Fig. 8 b), which suggests that perhaps these two sets of symptoms have independent mechanisms, with lethargy and fever caused by HOIL-1L–dependent inflammation and weight loss being due to an as yet unidentified factor. The HOIL-1L–dependent assembly of the NLRP3 inflammasome and linear ubiquitination of ASC likely contribute to the resistance of the HOIL-1L$^{-/-}$ mice upon LPS challenge because mice lacking functional NLRP3 inflammasomes or ASC are also resistant to LPS challenge (Mariathasan et al., 2004, 2006). Furthermore, the MDP-induced peritonitis model confirmed that HOIL-1L is indeed important for NLRP3 inflammasome activation in vivo (Fig. 7). Altogether, our data indicates that the regulation of inflammasome activation is achieved through complex ubiquitin linkage codes that in turn may have distinct consequences in response to stimuli. Our work has identified new members of a growing network of ubiquitin-mediated regulation, which is an increasingly appreciated mechanism for PRR signaling pathways.

MATERIALS AND METHODS

Mice. WT C57BL/6 mice were purchased from Charles River. HOIL-1L$^{-/-}$ mice have been previously described and were bred as homozygotes (Inn et al., 2011). For BMDM isolation, 6–8-wk-old male mice were sacrificed and BM cells were frozen as previously described (Marim et al., 2010). For MDP experiments, 7–10-wk-old female age-matched mice were injected in the i.p. cavity with 1 mg MDP (Sigma-Aldrich) in 100 µl PBS. 5 h after injection, a 1-ml PBS wash of the i.p. cavity was collected. Cells were pelleted from this wash for flow cytometry and supernatants were probed for cytokines by ELISA. For sepsis experiments, 6–14-wk-old age-matched and sex-matched mice were injected in the i.p. cavity with 30 mg/kg ultrapure LPS (*Escherichia coli* 0111:B4; Sigma-Aldrich) suspended in PBS and animals were monitored twice daily. Mice were given DietGel 76A supplemental liquid food at the beginning of weight loss. Mice were euthanized if they did not respond, were immobile, or lost >25% body mass. Survivors were euthanized 1 wk after the i.p. injection. For serum cytokine and spleen collection, animals were euthanized 24 h after i.p. injection. All animal protocols were performed in accordance with the approval of the USC Institutional Animal Care and Use Committee.

BMDM cell culture, lentivirus infection, and stimulation. BM cells were thawed and plated at a density of 10^6/well of a 24-well plate in DMEM supplemented with 10% FCS, 100 U/ml penicillin, 100 µg/ml streptomycin, and 10% L929 culture supernatant. Cells were differentiated for 1 wk with a media change on day 4. For IP experiments, BMDMs were trypsinized and plated on 10-cm dishes on day 4 after thawing. Priming with 5 µg/ml LPS (*E. coli* 0127:B8; Sigma-Aldrich) was done overnight in fresh media on day 6 after thawing for all experiments. Stimulation with 10 µg/ml MDP (*N*-Acetylmuramyl-L-alanyl-D-isoflutamine hydrate; Sigma-Aldrich) was done for 1 h in DMEM followed by a 30-min pulse with 5 mM ATP (Sigma-Aldrich). Stimulation with 10 µM Nigericin (Sigma-Aldrich) was done for 4 h (for caspase-1 cleavage and IL-1β secretion experiments) or 2 h (for IP and ASC foci experiments) in DMEM after overnight priming with 5 µg/ml LPS. Stimulation with 200 µg/ml silica or MSU (InvivoGen) was done during the last 8 h of the 11-h priming with LPS treatment. Stimulation with dsDNA was done for 4 h after LPS priming by Lipofectamine 2000 (Life Technologies)–mediated transfection with pEGFP-N1 (Takara Bio Inc.) vector DNA at a ratio of 1.5 µg DNA to 2 µl lipofectamine per well of a 24-well plate. Cells were stimulated with flagellin by infection at MOI 300 with Ad5-Flagellin or Ad5 control adenoviruses for 24 h after LPS priming. Cells were stimulated with *L. pneumophila* at MOI 1 or 10 for 2 h. Adenoviruses were a gift from S.-Y. Chen (University of Southern California) and *L. pneumophila* stocks were a gift from F. Shao (National Institute of Biological Sciences, Beijing, China). Lentiviruses were produced in 293T cultured in DMEM supplemented with 10% FCS, 100 U/ml penicillin, and 100 µg/ml streptomycin using the pCDH-CMV-MCS-EF1-puro system (System Biosciences) and standard calcium phosphate transfection. BMDMs were infected with lentivirus on day 3 or 4 after thawing in 24-well plates. BMDMs were infected by centrifugation for 30 min at 2,000 rpm in fresh media containing 8 µg/ml polybrene and 60–100 µl of virus stock per well as determined by titration of lentiviruses for equal protein expression. The inoculum was exchanged for fresh media after overnight incubation. Stimulations of lentivirus-infected BMDM were performed 7 d after thawing cells.

Microarray hybridization and analysis. RNA was isolated from BMDMs cultured in 10-cm dishes and treated with media alone, 10 ng/ml LPS, or 1 ng/ml TNF for 4 h on day 7 of differentiation. RNA was prepared by an RNeasy kit (QIAGEN). For each condition, 2 separate 10-cm dishes were used to generate 2 separate RNA preparations, $n = 2$. 8 × 60k array hybridizations (Agilent Technologies) were performed by UCLA Clinical Microarray Core according to standard protocol. Data were analyzed using the Genomics Suite (6.4; Partek). We used the RMA algorithm for data normalization. Thresholds for selecting significant genes were set at twofold or greater and FDR $P < 0.05$. Genes met both criteria simultaneously were considered as significant changes. NF-κB pathway analyses were performed using Ingenuity Pathway Analysis (Ingenuity Systems). The complete microarray dataset is accessible at NCBI GEO (GSE57180).

qRT-PCR. RNA was isolated from BMDM or MEF cells with 1 ml Tri Reagent (Sigma-Aldrich) and treated with 1 U RNase free DNase I (Sigma-Aldrich). cDNA was generated from 250 ng of total RNA (iScript; Bio-Rad Laboratories), diluted 1:10 with nuclease-free water, and quantified by real-time qPCR using the iQ SYBR Green Supermix kit (Bio-Rad Laboratories), according to the manufacturer's instructions. Reactions were cycled and analyzed on a CFX96 PCR machine (Bio-Rad Laboratories). Cycling conditions were a single step at 95°C for 5 min, followed by 40 cycles of 95°C for 15 s and 60°C for 30 s, followed by melt curve analysis. Primer sequences are summarized in Table S3. Threshold cycle (Ct) ratios were determined by normalizing to 18S RNA and a WT control sample using the following equation: relative expression = $100*2^{-(\Delta\Delta Ct)}$, where $\Delta\Delta Ct = (Ct_{gene} - Ct_{18S}) - (\Delta Ct_{WT\ unstimulated})$.

Cytokine quantification. Cytokines in cell culture supernatants were quantified by mouse IL-6 (BD) and mouse IL-1β ELISA kits (eBioscience). IL-1β levels in mouse sera were quantified using a custom multiplexing Milliplex MAP mouse cytokine assay (Millipore) and analyzed on a Bio-Plex plate reader using Bio-Plex Manager software (Bio-Rad Laboratories) at the USC Norris Immune Monitoring Core.

Flow cytometry. Cell pellets from mouse IP washes were stained with Ly6G-PE and cd11b-APC antibodies (BioLegend) at a dilution of 1:250. Flow cytometry was performed on a FACS Canto II (BD) followed by analysis using FlowJo software (Tree Star).

IP. 293T cells were transfected with cesium chloride purified preparations DNA plasmids by PEI as previously described (Inn et al., 2011). Cell lysates were collected 24 h after transfection in linear ubiquitination IP buffer (LUIP: 5M Urea, 135 mM NaCl, 1% Triton X-100, 1.5 mM $MgCl_2$, 2 mM *N*-ethyl maleimide, and complete protease inhibitor cocktail [Roche]). For BMDM experiments, cells were thawed in non-TC–treated dishes and cultured for 7 d in the presence of 10% L929. Cells were plated on TC-coated 10-cm dishes on day 4 after thawing and one dish was used per condition. Cell lysates were collected in IP buffer (1% NP-40, 50 mM Tris, pH 7.4, 150 mM NaCl, 0.5% sodium deoxycholate, and complete protease inhibitor cocktail [Roche]) and sonicated for 20 s at 10%. Lysates were precleared and incubated with antibody overnight at 4°C (IP) or room temperature (LUIP).

For LUIP, 0.25 µg of antibody was used (Genentech) per 10-cm dish of cells. For BMDM IPs, 2 µg rabbit antibody was used for ASC (Santa Cruz Biotechnology, Inc.). Protein A/G beads were incubated with lysate/antibody mixtures for 2 h before washing 3 times in IP buffer or 2 times in LUIP buffer followed by 2 PBS washes. IP beads were boiled in 2× Laemmli dye for 10 min and LUIP beads were incubated at 70°C for 10 min in LDS dye (Invitrogen) supplemented with fresh 5 mM DTT to elute protein complexes for Western blotting.

Immunoblotting. Cell lysates were collected in RIPA buffer (IP buffer + 0.1% SDS) and quantified by Bradford protein assay (Thermo Fisher Scientific). Proteins were separated by SDS-PAGE and transferred to PVDF membrane (Bio-Rad Laboratories) by semi-dry transfer at 25V for 30 min. For linear ubiquitin Western blots, SDS-PAGE was transferred to nitrocellulose (Bio-Rad Laboratories) by wet transfer at 4°C for 2 h at 30V. All membranes were blocked in 5% milk in PBST and probed overnight with indicated antibodies in 3% BSA, except for the linear ubiquitin antibody, which was incubated at room temperature for 1 h. Primary antibodies included: mouse IκBα (1:1,000; Cell Signaling Technology), mouse IL-1β (1:1,000; R&D), mouse caspase-1 (Santa Cruz Biotechnology, Inc.), actin (clone C4; Santa Cruz Biotechnology, Inc.), ASC (1:1,000; Santa Cruz Biotechnology, Inc.), human HOIP (1:250; Acris), V5 (1:2,000; Life Technologies), Flag (1:2,000; Sigma-Aldrich), and HA (1:2,000; Covance). Antibodies against HOIL-1L have been previously described (Tokunaga and Iwai, 2009). The linear ubiquitin antibody was a gift from Genentech and has been previously characterized in detail (Matsumoto et al., 2012). In brief, samples for linear ubiquitin immunoblots were separated by SDS-PAGE and transferred to nitrocellulose by wet transfer at 4°C, 30V, for 2 h. Membranes were blocked in 5% milk in PBST, probed with primary antibody (1:2,000) for 1 h at room temperature, washed, probed with TrueBlot-HRP (1:300; Thermo Fisher Scientific), and then developed with ECL (Thermo Fisher Scientific). For all other antibodies, appropriate HRP-conjugated secondary antibodies were incubated on membranes and bands were developed with ECL reagent (Thermo Fisher Scientific) and imaged on an LAS-4000 imager (Fuji). For IP with Western blots, the Clean Blot HRP secondary (1:300; Thermo Fisher Scientific) was substituted.

Immunofluorescence. FAM-YVAD-FLICA (FLICA; ImmunoChemistry Technologies) was reconstituted and diluted according to the manufacturer's instructions. FLICA was added to cells in DMEM containing 10 µg/µl MDP and 10% L929. 300 µl of this solution was added per well of a 24-well plate containing BMDM. After 2 h, ATP was added to the media at a concentration of 2.5 mM. 30 min later, the supernatant was removed and the cells were washed three times with PBS. The fixative provided by the manufacturer was added to the cells for 15 min at room temperature. For antibody staining, cells were fixed with methanol, washed three times, and permeabilized with 0.1% Triton X-100 for 10 min at room temperature. Blocking buffer (3% BSA in PBS) was applied for 1 h. Cells were incubated with anti–Caspase-1 (1:100; Santa Cruz Biotechnology, Inc.), anti-linear ubiquitin (1F11/3F5/Y102L, 1 µg/ml; Genentech), anti-ASC (AL177, 1:100; Enzo), and/or anti-HA (MMS-101P, 1:500; Covance) for 1 h. Cells were washed three times in PBS and incubated with Alexa Fluor–coupled secondary antibodies (1:500; Invitrogen) for 1 h. Cells were washed three times in PBS and incubated with Hoechst stain (1:1,000; Molecular Probes) for 10 min. Cells were mounted in ProLong Gold Antifade media and imaged with a confocal microscope (LSM510; Carl Zeiss) equipped with an EC Plan-Apochromat 63×/1.4 oil objective or a Plan-Apochromat 100×/1.4 oil DIC objective. Images were processed using LSM 510 Version 4.2 SP1 acquisition software. Z-stack images were taken with a Plan-Apochromat 100×/1.4 oil DIC objective.

Immunohistochemistry. Spleens were fixed in 10% formalin and embedded in paraffin. Sectioning, hematoxylin, eosin, and Annexin V (1:50; Novus Biologicals) staining were performed by the USC Immunohistochemistry Core facility. Images were acquired on a microscope (IX71; Olympus) using the 10× (Plan C 10×/0.25 PhC; Olympus) and 40× (SLC Plan F1 40×/0.55 Ph2; Olympus) objectives as indicated with a Digital Sight DS-Fi1 camera (Nikon).

GST-CoZi pulldown. The CoZi domain of human Nemo (Lee et al., 2012) was cloned into the BamHI and XhoI sites of the pGEX-6P-1 vector and the R309A, R312A, E313A triple mutant was generated through standard serial PCR with mutant oligos. BL21 bacteria were transformed with WT and rre Cozi pGEX plasmids and protein expression was induced with 0.3 mM IPTG when cells reached OD_{600} 0.5. After 90 min, cells were pelleted and lysed in HEPES-CHAPS buffer (20 mM Hepes, pH 8.0, 200 mM NaCl, and 15 mM CHAPS) supplemented with a complete protease inhibitor cocktail (Roche). After sonication and removal of the pellet, lysates were precleared for 1 h with Sepharose beads (GE Healthcare) and then incubated with GST4b beads (GE Healthcare) for 2 h at 4°C. Beads were washed extensively in Hepes-CHAPS buffer and then IP buffer. In parallel, lysates from 293T cells transfected with pIRES-ASC-3xFlag, pCDNA3.1-HOIL-1L-HA, and pCDNA3.1-Myc-HOIP plasmids (or empty vector controls) as indicated were collected in IP buffer supplemented with complete protease inhibitor cocktail (Roche) and 2 mM *N*-ethylmaleimide (NEM; Sigma-Aldrich) and precleared for 1 h with GST4b beads (GE Healthcare). Finally, 293T lysates were incubated with WT or rre Cozi GST beads overnight at 4°C. Beads were washed in IP buffer and boiled in 2× Laemmli dye for Western blotting.

In vitro linear ubiquitination assay. ASC-Flag and NLRP3-Flag were purified from 293T cells by M2 beads (Sigma-Aldrich) in high salt buffer (500 mM NaCl, 1% NP-40, and 50 mM Tris, pH 8.0) and eluted with Flag peptide (Sigma-Aldrich), followed by 10 kD MWCO dialysis in excess TBS overnight. HOIL-1L-6xHIS and HOIP-6xHIS were cloned into the pET-duet-1 vector, coexpressed in BL21 DE3 RIPL (Agilent Technologies) bacteria, and purified from cultures grown in the presence of 0.2 mM $ZnCl_2$ and 0.5 mM IPTG at 16°C for 24 h. Cells were lysed in native buffer (50 mM Tris, PH 8.0, and 100 mM NaCl) and HOIL-1L/HOIP were co-purified on cobalt beads (Thermo Fisher Scientific) with 150 mM imidazole elution and overnight dialysis in lysis buffer. HOIL-1L/HOIP (LUBAC) purification preps were stored at 4°C and never frozen. E1 (Ube1), E2 (UbcH5c), and ubiquitin were purchased from Boston Biochem. In vitro linear ubiquitination assays contained 200 ng E1, 400 ng E2, 1 µg HOIL-1L/HOIP-6xHIS purification prep, 20 mM Tris, pH 7.5, 5 mM DTT, 5 mM $MgCl_2$, 2 mM MgATP (Boston Biochem), 10 µg ubiquitin, and 0.5 µg purified Flag-tagged substrate.

Deubiquitinase assay. Beads from one linear ubiquitin IP from 293T cells expressing HOIL-1L-HA, myc-HOIP, and ASC-V5 were split into three tubes that were treated with reaction buffer (20 mM Hepes, pH 8.0, 50 mM NaCl, 1 mM $MgCl_2$, and 5 mM β-mercaptoethanol), 0.8 µM Otulin (Boston Biochem), or 0.04 mg/ml AMSH (Boston Biochem) at 30°C for 1 h in a total volume of 25 µl. Samples were diluted to 1× LDS loading dye (Life Technologies) and analyzed by Western blotting.

Statistical analysis. All experiments were performed three times and a representative experiment is presented here, except for BMDM IPs, which were performed on lysates combined from several mice in two separate experiments. For experiments with statistical analysis, a two-tailed Student's *t* test and p-values of <0.05 were considered significant.

Online supplemental material. Table S1 lists transcripts with a lower abundance in HOIL-1L$^{-/-}$ BMDMs and Table S2 lists transcripts with a higher abundance in HOIL-1L$^{-/-}$ BMDMs. Table S3 lists the primers used for qPCR. Fig. S1 shows immunoblot and IP controls for the linear ubiquitin antibody. Video 1 shows the Z-stacks for Fig. 4 c. Online supplemental material is available at http://www.jem.org/cgi/content/full/jem.20132486/DC1.

We thank Drs. Vishva Dixit (Genentech), Junying Yuan (Harvard Medical School), Si-Yi Chen (University of Southern California), Feng Shao (National Institute of Biological Sciences, Beijing, China), and Blossom Damania (University of North Carolina at Chapel Hill) for reagents. We thank the USC Norris Comprehensive Cancer Center Beckman Center for Immune Monitoring for running the multiplex cytokine assay. We thank the USC Pathology Immunohistochemistry core for spleen sectioning and staining. We thank the Cell and Tissue Imaging Core of USC Research Center for Liver Diseases for providing microscopy services (National

Institutes of Health grants P30 DK048522 and S10 RR022508). Finally, we thank all of J. J.'s laboratory members for their discussions.

This work was partly supported by 1F32AI096698 (M.A. Rodgers); CA180779, CA082057, CA31363, CA115284, AI073099, AI083025, HL110609, GRL, Hastings Foundation, and Fletcher Jones Foundation (J.U. Jung); and CA156330 and AI029564 (J. Ting).

The authors declare no competing financial interests.

Submitted: 1 December 2013
Accepted: 4 June 2014

REFERENCES

Boisson, B., E. Laplantine, C. Prando, S. Giliani, E. Israelsson, Z. Xu, A. Abhyankar, L. Israël, G. Trevejo-Nunez, D. Bogunovic, et al. 2012. Immunodeficiency, autoinflammation and amylopectinosis in humans with inherited HOIL-1 and LUBAC deficiency. *Nat. Immunol.* 13:1178–1186. http://dx.doi.org/10.1038/ni.2457

Broz, P., J. von Moltke, J.W. Jones, R.E. Vance, and D.M. Monack. 2010. Differential requirement for Caspase-1 autoproteolysis in pathogen-induced cell death and cytokine processing. *Cell Host Microbe*. 8:471–483. http://dx.doi.org/10.1016/j.chom.2010.11.007

Bruey, J.M., N. Bruey-Sedano, F. Luciano, D. Zhai, R. Balpai, C. Xu, C.L. Kress, B. Bailly-Maitre, X. Li, A. Osterman, et al. 2007. Bcl-2 and Bcl-XL regulate proinflammatory caspase-1 activation by interaction with NALP1. *Cell*. 129:45–56. http://dx.doi.org/10.1016/j.cell.2007.01.045

Bryan, N.B., A. Dorfleutner, Y. Rojanasakul, and C. Stehlik. 2009. Activation of inflammasomes requires intracellular redistribution of the apoptotic speck-like protein containing a caspase recruitment domain. *J. Immunol.* 182:3173–3182. http://dx.doi.org/10.4049/jimmunol.0802367

Damgaard, R.B., U. Nachbur, M. Yabal, W.W. Wong, B.K. Fiil, M. Kastirr, E. Rieser, J.A. Rickard, A. Bankovacki, C. Peschel, et al. 2012. The ubiquitin ligase XIAP recruits LUBAC for NOD2 signaling in inflammation and innate immunity. *Mol. Cell*. 46:746–758. http://dx.doi.org/10.1016/j.molcel.2012.04.014

Damgaard, R.B., B.K. Fiil, C. Speckmann, M. Yabal, U. zur Stadt, S. Bekker-Jensen, P.J. Jost, S. Ehl, N. Mailand, and M. Gyrd-Hansen. 2013. Disease-causing mutations in the XIAP BIR2 domain impair NOD2-dependent immune signalling. *EMBO Mol Med*. 5:1278–1295. http://dx.doi.org/10.1002/emmm.201303090

Dostert, C., V. Pétrilli, R. Van Bruggen, C. Steele, B.T. Mossman, and J. Tschopp. 2008. Innate immune activation through Nalp3 inflammasome sensing of asbestos and silica. *Science*. 320:674–677. http://dx.doi.org/10.1126/science.1156995

Emmerich, C.H., A. Ordureau, S. Strickson, J.S. Arthur, P.G. Pedrioli, D. Komander, and P. Cohen. 2013. Activation of the canonical IKK complex by K63/M1-linked hybrid ubiquitin chains. *Proc. Natl. Acad. Sci. USA*. 110:15247–15252. http://dx.doi.org/10.1073/pnas.1314715110

Fernandes-Alnemri, T., J.-W. Yu, P. Datta, J. Wu, and E.S. Alnemri. 2009. AIM2 activates the inflammasome and cell death in response to cytoplasmic DNA. *Nature*. 458:509–513. http://dx.doi.org/10.1038/nature07710

Franchi, L., R. Muñoz-Planillo, and G. Núñez. 2012. Sensing and reacting to microbes through the inflammasomes. *Nat. Immunol.* 13:325–332. http://dx.doi.org/10.1038/ni.2231

Gerlach, B., S.M. Cordier, A.C. Schmukle, C.H. Emmerich, E. Rieser, T.L. Haas, A.I. Webb, J.A. Rickard, H. Anderton, W.W.L. Wong, et al. 2011. Linear ubiquitination prevents inflammation and regulates immune signalling. *Nature*. 471:591–596. http://dx.doi.org/10.1038/nature09816

Haas, T.L., C.H. Emmerich, B. Gerlach, A.C. Schmukle, S.M. Cordier, E. Rieser, R. Feltham, J. Vince, U. Warnken, T. Wenger, et al. 2009. Recruitment of the linear ubiquitin chain assembly complex stabilizes the TNF-R1 signaling complex and is required for TNF-mediated gene induction. *Mol. Cell*. 36:831–844. http://dx.doi.org/10.1016/j.molcel.2009.10.013

Hara, H., K. Tsuchiya, I. Kawamura, R. Fang, E. Hernandez-Cuellar, Y. Shen, J. Mizuguchi, E. Schweighoffer, V. Tybulewicz, and M. Mitsuyama. 2013. Phosphorylation of the adaptor ASC acts as a molecular switch that controls the formation of speck-like aggregates and inflammasome activity. *Nat. Immunol.* 14:1247–1255. http://dx.doi.org/10.1038/ni.2749

Hornung, V., F. Bauernfeind, A. Halle, E.O. Samstad, H. Kono, K.L. Rock, K.A. Fitzgerald, and E. Latz. 2008. Silica crystals and aluminum salts activate the NALP3 inflammasome through phagosomal destabilization. *Nat. Immunol.* 9:847–856. http://dx.doi.org/10.1038/ni.1631

Ikeda, F., Y.L. Deribe, S.S. Skånland, B. Stieglitz, C. Grabbe, M. Franz-Wachtel, S.J.L. van Wijk, P. Goswami, V. Nagy, J. Terzic, et al. 2011. SHARPIN forms a linear ubiquitin ligase complex regulating NF-κB activity and apoptosis. *Nature*. 471:637–641. http://dx.doi.org/10.1038/nature09814

Inn, K.-S., M.U. Gack, F. Tokunaga, M. Shi, L.-Y. Wong, K. Iwai, and J.U. Jung. 2011. Linear ubiquitin assembly complex negatively regulates RIG-I- and TRIM25-mediated type I interferon induction. *Mol. Cell*. 41:354–365. http://dx.doi.org/10.1016/j.molcel.2010.12.029

Iwai, K., and F. Tokunaga. 2009. Linear polyubiquitination: a new regulator of NF-κB activation. *EMBO Rep.* 10:706–713. http://dx.doi.org/10.1038/embor.2009.144

Iyer, S.S., Q. He, J.R. Janczy, E.I. Elliott, Z. Zhong, A.K. Olivier, J.J. Sadler, V. Knepper-Adrian, R. Han, L. Qiao, et al. 2013. Mitochondrial cardiolipin is required for Nlrp3 inflammasome activation. *Immunity*. 39:311–323. http://dx.doi.org/10.1016/j.immuni.2013.08.001

Joosten, L.A.B., F.L. Van De Veerdonk, A.G. Vonk, O.C. Boerman, M. Keuter, G. Fantuzzi, I. Verschueren, T. Van Der Poll, C.A. Dinarello, B.-J. Kullberg, et al. 2010. Differential susceptibility to lethal endotoxaemia in mice deficient in IL-1α, IL-1β or IL-1 receptor type I. *APMIS*. 118:1000–1007. http://dx.doi.org/10.1111/j.1600-0463.2010.02684.x

Juliana, C., T. Fernandes-Alnemri, S. Kang, A. Farias, F. Qin, and E.S. Alnemri. 2012. Non-transcriptional priming and deubiquitination regulate NLRP3 inflammasome activation. *J. Biol. Chem.* 287:36617–36622. http://dx.doi.org/10.1074/jbc.M112.407130

Kayagaki, N., M.T. Wong, I.B. Stowe, S.R. Ramani, L.C. Gonzalez, S. Akashi-Takamura, K. Miyake, J. Zhang, W.P. Lee, A. Muszyński, et al. 2013. Noncanonical inflammasome activation by intracellular LPS independent of TLR4. *Science*. 341:1246–1249. http://dx.doi.org/10.1126/science.1240248

Keusekotten, K., P.R. Elliott, L. Glockner, B.K. Fiil, R.B. Damgaard, Y. Kulathu, T. Wauer, M.K. Hospenthal, M. Gyrd-Hansen, D. Krappmann, et al. 2013. OTULIN antagonizes LUBAC signaling by specifically hydrolyzing Met1-linked polyubiquitin. *Cell*. 153:1312–1326. http://dx.doi.org/10.1016/j.cell.2013.05.014

Kirisako, T., K. Kamei, S. Murata, M. Kato, H. Fukumoto, M. Kanie, S. Sano, F. Tokunaga, K. Tanaka, and K. Iwai. 2006. A ubiquitin ligase complex assembles linear polyubiquitin chains. *EMBO J.* 25:4877–4887. http://dx.doi.org/10.1038/sj.emboj.7601360

Komander, D., F. Reyes-Turcu, J.D. Licchesi, P. Odenwaelder, K.D. Wilkinson, and D. Barford. 2009. Molecular discrimination of structurally equivalent Lys 63-linked and linear polyubiquitin chains. *EMBO Rep.* 10:466–473. http://dx.doi.org/10.1038/embor.2009.55

Kovarova, M., P.R. Hesker, L. Jania, M. Nguyen, J.N. Snouwaert, Z. Xiang, S.E. Lommatzsch, M.T. Huang, J.P.-Y. Ting, and B.H. Koller. 2012. NLRP1-dependent pyroptosis leads to acute lung injury and morbidity in mice. *J. Immunol.* 189:2006–2016. http://dx.doi.org/10.4049/jimmunol.1201065

Lee, S.H., Z. Toth, L.Y. Wong, K. Brulois, J. Nguyen, J.Y. Lee, E. Zandi, and J.U. Jung. 2012. Novel phosphorylations of IKKγ/NEMO. *MBio*. 3:e00411–e00412. http://dx.doi.org/10.1128/mBio.00411-12

Liang, Y. 2011. SHARPIN negatively associates with TRAF2-mediated NFκB activation. *PLoS ONE*. 6:e21696. http://dx.doi.org/10.1371/journal.pone.0021696

Liang, Y., R.E. Seymour, and J.P. Sundberg. 2011. Inhibition of NF-κB signaling retards eosinophilic dermatitis in SHARPIN-deficient mice. *J. Invest. Dermatol.* 131:141–149. http://dx.doi.org/10.1038/jid.2010.259

Lopez-Castejon, G., N.M. Luheshi, V. Compan, S. High, R.C. Whitehead, S.L. Flitsch, A. Kirov, I. Prudovsky, E. Swanton, and D. Brough. 2013. Deubiquitinases regulate the activity of caspase-1 and interleukin-1β secretion via assembly of the inflammasome. *J. Biol. Chem.* 288:2721–2733. http://dx.doi.org/10.1074/jbc.M112.422238

Mariathasan, S., K. Newton, D.M. Monack, D. Vucic, D.M. French, W.P. Lee, M. Roose-Girma, S. Erickson, and V.M. Dixit. 2004. Differential activation of

the inflammasome by caspase-1 adaptors ASC and Ipaf. *Nature*. 430:213–218. http://dx.doi.org/10.1038/nature02664

Mariathasan, S., D.S. Weiss, K. Newton, J. McBride, K. O'Rourke, M. Roose-Girma, W.P. Lee, Y. Weinrauch, D.M. Monack, and V.M. Dixit. 2006. Cryopyrin activates the inflammasome in response to toxins and ATP. *Nature*. 440:228–232. http://dx.doi.org/10.1038/nature04515

Marim, F.M., T.N. Silveira, D.S. Lima Jr., and D.S. Zamboni. 2010. A method for generation of bone marrow-derived macrophages from cryopreserved mouse bone marrow cells. *PLoS ONE*. 5:e15263. http://dx.doi.org/10.1371/journal.pone.0015263

Martinon, F., K. Burns, and J. Tschopp. 2002. The inflammasome: a molecular platform triggering activation of inflammatory caspases and processing of proIL-beta. *Mol. Cell*. 10:417–426. http://dx.doi.org/10.1016/S1097-2765(02)00599-3

Matsumoto, M.L., K.C. Dong, C. Yu, L. Phu, X. Gao, R.N. Hannoush, S.G. Hymowitz, D.S. Kirkpatrick, V.M. Dixit, and R.F. Kelley. 2012. Engineering and structural characterization of a linear polyubiquitin-specific antibody. *J. Mol. Biol.* 418:134–144. http://dx.doi.org/10.1016/j.jmb.2011.12.053

McNamara, M.J., J.A. Norton, R.J. Nauta, and H.R. Alexander. 1993. Interleukin-1 receptor antibody (IL-1rab) protection and treatment against lethal endotoxemia in mice. *J. Surg. Res.* 54:316–321. http://dx.doi.org/10.1006/jsre.1993.1050

Miao, E.A., D.P. Mao, N. Yudkovsky, R. Bonneau, C.G. Lorang, S.E. Warren, I.A. Leaf, and A. Aderem. 2010. Innate immune detection of the type III secretion apparatus through the NLRC4 inflammasome. *Proc. Natl. Acad. Sci. USA*. 107:3076–3080. http://dx.doi.org/10.1073/pnas.0913087107

Nakahira, K., J.A. Haspel, V.A.K. Rathinam, S.-J. Lee, T. Dolinay, H.C. Lam, J.A. Englert, M. Rabinovitch, M. Cernadas, H.P. Kim, et al. 2011. Autophagy proteins regulate innate immune responses by inhibiting the release of mitochondrial DNA mediated by the NALP3 inflammasome. *Nat. Immunol.* 12:222–230. http://dx.doi.org/10.1038/ni.1980

Nakamura, M., F. Tokunaga, S.-i. Sakata, and K. Iwai. 2006. Mutual regulation of conventional protein kinase C and a ubiquitin ligase complex. *Biochem. Biophys. Res. Commun.* 351:340–347. http://dx.doi.org/10.1016/j.bbrc.2006.09.163

Pan, Q., J. Mathison, C. Fearns, V.V. Kravchenko, J. Da Silva Correia, H.M. Hoffman, K.S. Kobayashi, J. Bertin, E.P. Grant, A.J. Coyle, et al. 2007. MDP-induced interleukin-1beta processing requires Nod2 and CIAS1/NALP3. *J. Leukoc. Biol.* 82:177–183. http://dx.doi.org/10.1189/jlb.1006627

Proell, M., M. Gerlic, P.D. Mace, J.C. Reed, and S.J. Riedl. 2013. The CARD plays a critical role in ASC foci formation and inflammasome signalling. *Biochem. J.* 449:613–621. http://dx.doi.org/10.1042/BJ20121198

Py, B.F., M.S. Kim, H. Vakifahmetoglu-Norberg, and J. Yuan. 2013. Deubiquitination of NLRP3 by BRCC3 critically regulates inflammasome activity. *Mol. Cell*. 49:331–338. http://dx.doi.org/10.1016/j.molcel.2012.11.009

Rahighi, S., F. Ikeda, M. Kawasaki, M. Akutsu, N. Suzuki, R. Kato, T. Kensche, T. Uejima, S. Bloor, D. Komander, et al. 2009. Specific recognition of linear ubiquitin chains by NEMO is important for NF-κB activation. *Cell*. 136:1098–1109. http://dx.doi.org/10.1016/j.cell.2009.03.007

Rathinam, V.A.K., Z. Jiang, S.N. Waggoner, S. Sharma, L.E. Cole, L. Waggoner, S.K. Vanaja, B.G. Monks, S. Ganesan, E. Latz, et al. 2010. The AIM2 inflammasome is essential for host defense against cytosolic bacteria and DNA viruses. *Nat. Immunol.* 11:395–402. http://dx.doi.org/10.1038/ni.1864

Rivkin, E., S.M. Almeida, D.F. Ceccarelli, Y.C. Juang, T.A. MacLean, T. Srikumar, H. Huang, W.H. Dunham, R. Fukumura, G. Xie, et al. 2013. The linear ubiquitin-specific deubiquitinase gumby regulates angiogenesis. *Nature*. 498:318–324. http://dx.doi.org/10.1038/nature12296

Sato, Y., H. Fujita, A. Yoshikawa, M. Yamashita, A. Yamagata, S.E. Kaiser, K. Iwai, and S. Fukai. 2011. Specific recognition of linear ubiquitin chains by the Npl4 zinc finger (NZF) domain of the HOIL-1L subunit of the linear ubiquitin chain assembly complex. *Proc. Natl. Acad. Sci. USA*. 108:20520–20525. http://dx.doi.org/10.1073/pnas.1109088108

Schroder, K., and J. Tschopp. 2010. The inflammasomes. *Cell*. 140:821–832. http://dx.doi.org/10.1016/j.cell.2010.01.040

Seok, J., H.S. Warren, A.G. Cuenca, M.N. Mindrinos, H.V. Baker, W. Xu, D.R. Richards, G.P. McDonald-Smith, H. Gao, L. Hennessy, et al., Inflammation and Host Response to Injury, Large Scale Collaborative Research Program. 2013. Genomic responses in mouse models poorly mimic human inflammatory diseases. *Proc. Natl. Acad. Sci. USA*. 110:3507–3512. http://dx.doi.org/10.1073/pnas.1222878110

Shenoy, A.R., D.A. Wellington, P. Kumar, H. Kassa, C.J. Booth, P. Cresswell, and J.D. MacMicking. 2012. GBP5 promotes NLRP3 inflammasome assembly and immunity in mammals. *Science*. 336:481–485. http://dx.doi.org/10.1126/science.1217141

Shi, C.S., K. Shenderov, N.N. Huang, J. Kabat, M. Abu-Asab, K.A. Fitzgerald, A. Sher, and J.H. Kehrl. 2012. Activation of autophagy by inflammatory signals limits IL-1β production by targeting ubiquitinated inflammasomes for destruction. *Nat. Immunol.* 13:255–263. http://dx.doi.org/10.1038/ni.2215

Shimada, K., T.R. Crother, J. Karlin, J. Dagvadorj, N. Chiba, S. Chen, V.K. Ramanujan, A.J. Wolf, L. Vergnes, D.M. Ojcius, et al. 2012. Oxidized mitochondrial DNA activates the NLRP3 inflammasome during apoptosis. *Immunity*. 36:401–414. http://dx.doi.org/10.1016/j.immuni.2012.01.009

Stieglitz, B., A.C. Morris-Davies, M.G. Koliopoulos, E. Christodoulou, and K. Rittinger. 2012. LUBAC synthesizes linear ubiquitin chains via a thioester intermediate. *EMBO Rep.* 13:840–846. http://dx.doi.org/10.1038/embor.2012.105

Tatematsu, K., C. Tokunaga, N. Nakagawa, K. Tanizawa, S. Kuroda, and U. Kikkawa. 1998. Transcriptional activity of RBCK1 protein (RBCC protein interacting with PKC 1): requirement of RING-finger and B-Box motifs and regulation by protein kinases. *Biochem. Biophys. Res. Commun.* 247:392–396. http://dx.doi.org/10.1006/bbrc.1998.8795

Tokunaga, F., and K. Iwai. 2009. [Involvement of LUBAC-mediated linear polyubiquitination of NEMO in NF-κB activation]. *Tanpakushitsu Kakusan Koso*. 54:635–642.

Tokunaga, C., S. Kuroda, K. Tatematsu, N. Nakagawa, Y. Ono, and U. Kikkawa. 1998. Molecular cloning and characterization of a novel protein kinase C-interacting protein with structural motifs related to RBCC family proteins. *Biochem. Biophys. Res. Commun.* 244:353–359. http://dx.doi.org/10.1006/bbrc.1998.8270

Tokunaga, F., S.-i. Sakata, Y. Saeki, Y. Satomi, T. Kirisako, K. Kamei, T. Nakagawa, M. Kato, S. Murata, S. Yamaoka, et al. 2009. Involvement of linear polyubiquitylation of NEMO in NF-κB activation. *Nat. Cell Biol.* 11:123–132. http://dx.doi.org/10.1038/ncb1821

Tokunaga, F., T. Nakagawa, M. Nakahara, Y. Saeki, M. Taniguchi, S.-i. Sakata, K. Tanaka, H. Nakano, and K. Iwai. 2011. SHARPIN is a component of the NF-κB-activating linear ubiquitin chain assembly complex. *Nature*. 471:633–636. http://dx.doi.org/10.1038/nature09815

Tokunaga, F., H. Nishimasu, R. Ishitani, E. Goto, T. Noguchi, K. Mio, K. Kamei, A. Ma, K. Iwai, and O. Nureki. 2012. Specific recognition of linear polyubiquitin by A20 zinc finger 7 is involved in NF-κB regulation. *EMBO J.* 31:3856–3870. http://dx.doi.org/10.1038/emboj.2012.241

Verhelst, K., I. Carpentier, M. Kreike, L. Meloni, L. Verstrepen, T. Kensche, I. Dikic, and R. Beyaert. 2012. A20 inhibits LUBAC-mediated NF-κB activation by binding linear polyubiquitin chains via its zinc finger 7. *EMBO J.* 31:3845–3855. http://dx.doi.org/10.1038/emboj.2012.240

Wertz, I.E., K.M. O'Rourke, H. Zhou, M. Eby, L. Aravind, S. Seshagiri, P. Wu, C. Wiesmann, R. Baker, D.L. Boone, et al. 2004. De-ubiquitination and ubiquitin ligase domains of A20 downregulate NF-κB signalling. *Nature*. 430:694–699. http://dx.doi.org/10.1038/nature02794

Zak, D.E., F. Schmitz, E.S. Gold, A.H. Diercks, J.J. Peschon, J.S. Valvo, A. Niemistö, I. Podolsky, S.G. Fallen, R. Suen, et al. 2011. Systems analysis identifies an essential role for SHANK-associated RH domain-interacting protein (SHARPIN) in macrophage Toll-like receptor 2 (TLR2) responses. *Proc. Natl. Acad. Sci. USA*. 108:11536–11541. http://dx.doi.org/10.1073/pnas.1107577108

Zhao, Y., J. Yang, J. Shi, Y.-N. Gong, Q. Lu, H. Xu, L. Liu, and F. Shao. 2011. The NLRC4 inflammasome receptors for bacterial flagellin and type III secretion apparatus. *Nature*. 477:596–600. http://dx.doi.org/10.1038/nature10510